

## RESSALVA

Atendendo solicitação do(a)  
autor(a), o texto completo desta tese  
será disponibilizado somente a partir  
de 25/11/2016.

## TH SE DE DOCTORAT

DE

UNIVERSIDADE ESTADUAL PAULISTA “J LIO DE MESQUITA FILHO”,  
FACULDADE DE CI NCIAS FARMAC UTICAS

ET DE

L’UNIVERSIT  PARIS-SACLAY, L’UNIVERSIT  PARIS SUD

Programa de P s-gradua  o em Ci ncias Farmac uticas

 COLE DOCTORALE N 569-Innovation Th rapeutique, du fondamental   l’appliqu 

Doutorado em Ci ncias Farmac uticas

Sp cialit  de doctorat : Pharmacotechnie et biopharmacie

Par

**Mlle Elo sa Berbel Manaia**

Zinc oxide (ZnO) based quantum dots for bioimaging applications of lipid nanocarriers

Conception de Quantum dots   base d’oxyde de zinc (ZnO) pour des applications en  
bio-imagerie de nanosyst mes lipidiques

Pontos Qu nticos   base de  xido de zinco (ZnO) para aplica  es em bioimagem de  
nanocarreadores lip dicos

**Th se pr sent e et soutenue   Araraquara, le 25may 2016:**

**Dir cteurs de th se:**

Mme Claudie Bourgaux, Charg e de recherche, Universit  Paris-Sud, Directeur de th se

Mme Leila Aparecida Chiavacci Favorin, Professeur, UNESP-FCFAR, Directeur de th se

Mme Renata C. K. Kaminski, Professeur, UFS, Co-Directeur de th se

**Composition du Jury:**

M. Celso V. Santilli, Professeur, UNESP-IQ, Examineur

Mme. Am lie Bochot, Professeure, Universit  Paris-Sud, Pr sident du Jury

M. Damien Boyer, Ma tre de Conf rences, SIGMA Clermont, Rapporteur

Mme. M rcia Carvalhode Abreu Fantini, Professeure, USP-IF, Rapporteur

Araraquara – SP

2016

THÈSE DE DOCTORAT  
DE

UNIVERSIDADE ESTADUAL PAULISTA “JÚLIO DE MESQUITA FILHO”,  
FACULDADE DE CIÊNCIAS FARMACÊUTICAS

ET DE

L'UNIVERSITE PARIS-SACLAY, L'UNIVERSITE PARIS SUD

Programa de Pós-graduação em Ciências Farmacêuticas

ÉCOLE DOCTORALE N°569 - Innovation Thérapeutique, du fondamental à  
l'appliqué

Doutorado em Ciências Farmacêuticas

Spécialité de doctorat : Pharmacotechnie et biopharmacie

Par

**Mlle Eloísa Berbel Manaia**

Zinc oxide (ZnO) based quantum dots for bioimaging applications of lipid nanocarriers

Conception de Quantum dots à base d'oxyde de zinc (ZnO) pour des applications en  
bio-imagerie de nanosystèmes lipidiques

Pontos Quânticos à base de óxido de zinco (ZnO) para aplicações em bioimagem de  
nanocarreadores lipídicos

**Dirécteurs de thèse:**

Mme Claudie Bourgaux, Chargée de recherche, Université Paris-Sud, Directeur de thèse

Mme Leila Aparecida Chiavacci Favorin, Professeur, UNESP-FCFAR, Directeur de thèse

Mme Renata C. K. Kaminski, Professeur, UFS, Co-Directeur de thèse

Tese apresentada ao programa de Pós Graduação em Ciências Farmacêuticas, Área de Pesquisa e Desenvolvimento de Fármacos e Medicamentos, da Faculdade de Ciências Farmacêuticas, Universidade Estadual Paulista Júlio de Mesquita Filho, como parte dos requisitos para obtenção do título de Doutora em Ciências Farmacêuticas.

Araraquara – SP  
2016

**Ficha Catalográfica**

Elaborada Pelo Serviço Técnico de Biblioteca e Documentação  
Faculdade de Ciências Farmacêuticas  
UNESP – Campus de Araraquara

**M266p** Manaia, Eloísa Berbel  
Pontos Quânticos à base de óxido de zinco (ZnO) para aplicações em bioimagem de nanocarreadores lipídicos / Eloísa Berbel Manaia. – Araraquara, 2016  
175 f.

Tese (Doutorado) – Universidade Estadual Paulista. "Júlio de Mesquita Filho". Faculdade de Ciências Farmacêuticas. Programa de Pós Graduação em Ciências Farmacêuticas

Orientador: Leila Aparecida Chiavacci Favorin  
Orientador no exterior: Claudie Bourgaux  
Coorientador: Renata Cristina Kiatkoski Kaminski

1. ZnO. 2. Pontos quânticos. 3. Bioimagem. 4. Nanocarreadores lipídicos. I. Favorin, Leila Aparecida Chiavacci, orient. II. Bourgaux, Claudie, orient. III. Kaminski, Renata Cristina Kiatkoski, coorient. IV. Título.

**CAPES: 40300005**

**ELOÍSA BERBEL MANAIA**

**PONTOS QUÂNTICOS À BASE DE ÓXIDO DE ZINCO (ZnO) PARA  
APLICAÇÕES EM BIOIMAGEM DE NANOCARREADORES LIPÍDICOS**

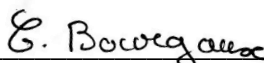
Tese de Doutorado apresentada à Faculdade de  
Ciências Farmacêuticas da Universidade Estadual  
Paulista – UNESP, Campus de Araraquara como  
requisito para a obtenção do título de Doutor em  
Ciências Farmacêuticas

Araraquara, 25 de maio de 2016.

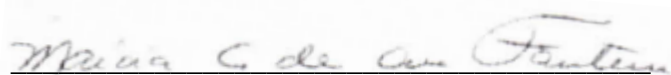
**BANCA EXAMINADORA**



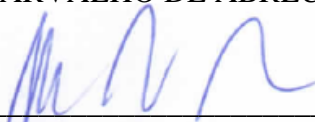
LEILA APARECIDA CHIAVACCI FAVORIN (Orientadora)



CLAUDIE BOURGAUX



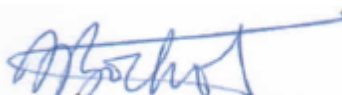
MÁRCIA CARVALHO DE ABREU FANTINI



CELSO VALENTIM SANTILLI



DAMIEN BOYER



AMÉLIE BOCHOT

**Title :** Zinc oxide (ZnO) based quantum dots for bioimaging applications of lipid nanocarriers

**Keywords :** ZnO, Quantum Dots, bioimaging, and lipid nanocarriers

**Abstract:** Theranostic systems consist of a single device containing therapeutics and diagnosis agents and have increased attention in the actual researches because these devices can improve the disease therapy such as cancer, decrease the side effects and the toxicity in non-cancer cells and permit monitoring the treatment. The aim of this work was to develop theranostic systems consisted of lipid based nanocarriers containing ZnO based quantum dots (QDs) as cancer cell luminescent guides, and a model drug for cancer therapy. Firstly, it was study the synthesis of ZnO/ZnS QDs aiming to achieve improved luminescent properties. In this step, X-Rays Absorption Spectroscopy, together with other usual characterization techniques, could identify the synthesis condition in which core-shell structures were formed. Nevertheless, the emission of ZnO/ZnS QDs in the visible range was not promising. Therefore, Mg-doped ZnO QDs were synthesized and their luminescence went through a maximum for a 20 mol% nominal concentration of  $Mg^{2+}$  ions in the reaction medium.  $Zn_{0.8}Mg_{0.2}O$  QDs presented quantum yield (QY) six times higher (QY = 64%) than undoped ones (QY = 10%). ZnO and  $Zn_{0.8}Mg_{0.2}O$  QDs capped by oleic acid (OA) were synthesized and formed stable colloidal dispersions in chloroform and toluene. The QY of OA- $Zn_{0.8}Mg_{0.2}O$  was about 4 times (around 40%) higher than that of the OA-ZnO QDs.  $Zn_{0.8}Mg_{0.2}O$  QDs and OA- $Zn_{0.8}Mg_{0.2}O$  QDs could be incorporated into lipid based nanocarriers of average hydrodynamic diameter around 100 – 220 nm. The luminescent solid lipid nanoparticles (SLN) were stable in different media at 37°C during 3 hours. The fluorescence association study showed enhanced emission of the J774 macrophage-like cells treated with 2 mg/mL of luminescent SLN during 50 min, suggesting partial internalization of the nanoparticles into the macrophages. The internalization study using the video-microscope and fluorescence microscope were not successfully, once the equipment condition used could not overcome the cells auto-fluorescence phenomena.

**Titre :** Conception de Quantum dots à base d'oxyde de zinc (ZnO) pour des applications en bio-imagerie de nanosystèmes lipidiques

**Mots clés :** ZnO, Quantum Dots, bioimagerie et nanosystèmes lipidiques

**Résumé :** Les systèmes théranostiques sont constitués d'un dispositif unique contenant des agents thérapeutiques et diagnostiques et attirent actuellement l'attention pour améliorer le traitement de maladies telles que le cancer ; ils pourraient réduire les effets secondaires (e.g. la toxicité pour les cellules non-cancéreuses) et permettre le suivi du traitement. Les quantum dots (QDs) sont utilisés comme agents d'imagerie *in vitro* et *in vivo*. Parmi ceux-ci, ZnO est moins cher, plus biocompatible et moins toxique que ceux utilisés couramment (SeCd, PbS, etc.). Le but de notre étude était de développer des systèmes théranostiques constitués de nanoparticules lipidiques contenant des QDs à base de ZnO comme agent luminescent, l'objectif final étant d'incorporer un principe actif pour le traitement du cancer. Nous avons d'abord étudié la synthèse de QDs de ZnO/ZnS (structure coeur/coquille) par le procédé sol-gel, afin d'améliorer les propriétés de luminescence de ZnO grâce à la passivation de la surface par le ZnS. Pour cela, deux voies de synthèse ont été explorées: le thioacétamide (TAA), utilisé comme source d'ions soufre, a été ajouté à (i) la solution de précurseur de l'acétate de zinc, et (ii) la suspension colloïdale de ZnO. Différentes concentrations de thioacétamide (TAA) ont été utilisées (1,5, 5 et 50 mM). Pour distinguer la formation de la structure coeur/coquille (ZnO / ZnS) d'un simple mélange de particules de ZnO et ZnS, les échantillons ont été caractérisés par plusieurs techniques (DRX, XAS, SAXS, UV-vis, pH, HRTEM et PL). Parmi celles-ci, l'absorption des rayons X (XAS) a été essentielle pour montrer que seule la réaction effectuée à partir de la suspension colloïdale de ZnO contenant 5 mM de TAA donnait lieu à la structure ZnO/ZnS. Cependant, les QDs de ZnO/ZnS n'ont pas montré une intensité de l'émission dans le visible plus grande que celle des QDs de ZnO. Les QDs de ZnO ont donc été dopés pour générer des électrons ou des trous supplémentaires dans leur structure, entraînant des changements de leurs propriétés de luminescence. Différentes quantités de Mg (2,5, 5, 10 et 20% en mole) ont été ajoutées lors

de la synthèse du ZnO par la voie sol-gel, afin d'obtenir des particules ayant une luminescence plus forte dans le visible. Plusieurs techniques (XRD, HRTEM, ICP-MS, SAXS, UV-Vis et PL) ont été utilisées pour déterminer les caractéristiques physico-chimiques des différents  $Zn_{1-x}Mg_xO$  QDs obtenus. Il a été observé une diminution de la taille des particules avec l'augmentation de la concentration de Mg. Lors de l'ajout d'une concentration nominale de  $Mg^{2+}$  dans le milieu réactionnel de 20% molaire ( $Zn_{0,8}Mg_{0,2}O$ ), le rendement quantique (QY) était six fois plus élevé (QY= 64%) que celui de la suspension de ZnO non dopé (QY= 10%). Pour utiliser les QDs dans un environnement biologique tout en conservant leurs propriétés de photoluminescence, leur surface est généralement modifiée par des substances hydrophiles pour les rendre stables dans l'eau, ou des substances hydrophobes pour permettre leur intégration dans des systèmes/nanoparticules à base de lipides ou de polymères. La surface des QDs de ZnO et  $Zn_{0,8}Mg_{0,2}O$  a été recouverte par de l'acide oléique (AO) ; les QDs ainsi modifiés forment une dispersion colloïdale stable dans le chloroforme et le toluène. La spectroscopie Raman a confirmé la présence d'acide oléique à la surface des QDs. Le rendement quantique des QDs de  $Zn_{0,8}Mg_{0,2}O$  recouverts d'AO était environ 4 fois plus élevé (QR = 40%) que celui des QDs de ZnO recouverts d'AO. Enfin, les QDs de  $Zn_{0,8}Mg_{0,2}O$ , recouverts ou non d'AO, ont été incorporés dans des nanoparticules lipidiques pour une utilisation ultérieure dans des études d'internalisation cellulaire. Des formulations à base de DPPC, DSPE-Peg et des nanoparticules lipidiques solides (SLN) contenant des QDs ont été préparées avec une taille hydrodynamique variant entre 100 et 220 nm. Les formulations à base de DSPE-Peg ont montré une intensité d'émission plus élevée dans le visible, comparé aux SLNs. L'étude de stabilité réalisée avec des SLNs luminescentes dans différents milieux (eau, PBS, PBS avec du Mg et du Ca, RPMI avec du sérum à 10%) à 37°C pendant 3 heures a montré que la taille ne changeait pas

fortement au cours du temps. Dans cette étude, la taille maximale était de l'ordre de 300 nm, montrant que même en présence de protéines, il ne se forme pas de gros agrégats. Trois méthodes ont été utilisées pour l'étude de l'internalisation cellulaire dans des macrophages J774. Lorsque la longueur d'onde d'excitation correspond à celle des QDs, les mesures d'intensité de fluorescence sur les suspensions de cellules ont montré une faible augmentation de l'intensité de l'émission visible pour les cellules incubées avec 2 mg/mL de SLNs luminescentes pendant 50 minutes, en comparaison avec les cellules témoins. Ce résultat suggère une internalisation partielle des SLNs dans les macrophages. Malheureusement, ces résultats n'ont pas pu être confirmés par vidéo-microscopie et

microscopie de fluorescence sur les cellules parce que les conditions expérimentales (longueurs d'onde d'excitation et d'émission possibles) ne permettaient pas d'observer un signal supérieur à celui de l'auto-fluorescence des cellules.

En conclusion, cette étude a permis d'optimiser la composition et la synthèse par voie sol-gel de QDs à base de ZnO pour les rendre aptes à être utilisés comme sondes luminescentes dans des nanoparticules lipidiques. La relation entre leur structure et leurs propriétés de luminescence a été étudiée; les QDs dopés  $Zn_{0.8}Mg_{0.2}O$ , qui ont le rendement quantique le plus élevé, ont pu être incorporés dans des nanoparticules lipidiques pouvant contenir des agents thérapeutiques.



**Título :** Pontos Quânticos à base de óxido de zinco (ZnO) para aplicações em bioimagem de nanocarreadores lipídicos

**Palavras-chaves :** ZnO, Pontos Quânticos, bioimagem e nanocarreadores lipídicos

**Resumo :** Sistemas teranósticos consistem em um único dispositivo contendo agentes terapêuticos e de diagnóstico e tem ganhado atenção nas pesquisas atuais por melhorar o tratamento de doenças como câncer, podendo diminuir efeitos colaterais, diminuir toxicidade em células não cancerígenas e permitir o monitoramento do tratamento. Os pontos quânticos (PQs) vem sendo usado como agentes de imagem para realizar o monitoramento ótico em investigações *in vivo* e *in vitro*. Dentre eles, o ZnO tem se destacado por ser mais barato, mais biocompatível e menos tóxico do que os utilizados comumente (SeCd, PbS, etc). O objetivo deste trabalho foi desenvolver sistemas teranósticos constituídos de nanocarreadores à base de lipídeos contendo pontos quânticos a base de ZnO, como guias luminescentes de células cancerígenas, e um fármaco modelo para tratamento do câncer. Primeiramente, foi estudada a síntese de pontos quânticos de ZnO/ZnS (estrutura de casca/caroço) pelo processo sol-gel, a fim de melhorar as propriedades luminescentes do ZnO através da passivação da sua superfície provocada pelo ZnS. Para isto, as reações de síntese tiveram como base (i) a solução precursora de acetato de Zinco e (ii) a suspensão coloidal de ZnO. Além disso, foram variadas as concentrações de tioacetamida (TAA) (1.5, 5 e 50mM), usada como fonte de íons de enxofre. Para diferenciar a formação de estruturas casca/caroço (ZnO/ZnS) e não uma mistura de partículas de ZnO e ZnS, várias técnicas foram utilizadas para caracterizar as amostras (DRX, XAS, SAXS, UV-vis, pH, HRTEM e PL). Dentre elas, XAS foi crucial para identificar que somente a reação realizada a partir da suspensão coloidal de ZnO com TAA 5mM deu origem à estrutura de ZnO/ZnS do tipo casca/caroço. Entretanto, os PQs de ZnO/ZnS não apresentaram maior intensidade da emissão na região do visível quando comparado ao ZnO. Portanto, PQs de ZnO foram dopados com Mg para gerar elétrons ou buracos extras na sua estrutura levando a mudanças em suas propriedades luminescentes. Diferentes quantidades de Mg (2.5, 5, 10 e 20

% em mol) foram usadas durante a síntese de ZnO pelo processo sol-gel para poder obter, assim, partículas com maior luminescência na região do visível. DRX, HRTEM, ICP-MS, SAXS, UV-Vis e PL foram usadas a fim de avaliar as características físico-químicas dos diferentes  $Zn_{1-x}Mg_xO$  obtidos. Observou-se a diminuição do tamanho das partículas com o aumento da concentração de Mg. Quando se utilizou 20 % em mols em concentração nominal de íons  $Mg^{2+}$  no meio reacional ( $Zn_{0.8}Mg_{0.2}O$ ), o rendimento quântico (RQ) foi seis vezes maior (RQ = 64%) do que a suspensão de ZnO não dopado (RQ = 10%). Para utilizar os PQs em meio biológico mantendo sua propriedade fotoluminescente, sua superfície normalmente é modificada com substâncias hidrofílicas para torná-los estáveis em água, ou com substâncias hidrofóbicas para permitir sua incorporação em sistemas/carreadores à base de lipídeos ou polímeros. Os PQs de ZnO e de  $Zn_{0.8}Mg_{0.2}O$  foram revestidos com ácido oleico (AO) formando uma dispersão coloidal estável em clorofórmio e tolueno. A espectroscopia RAMAN permitiu confirmar a modificação da superfície dos PQs pela presença dos grupamentos característicos do AO nessas amostras. O RQ do  $Zn_{0.8}Mg_{0.2}O$  revestido com AO foi em torno de 4 vezes maior (RQ = 40%) que o RQ de ZnO revestido com AO. Por fim, os PQs de  $Zn_{0.8}Mg_{0.2}O$  revestidos e não-revestidos com AO foram incorporados em nanocarreadores lipídicos para serem utilizados posteriormente nos estudos de internalização celular. Formulações à base de DPPC, DSPE-Peg e nanopartículas lipídicas sólidas (NLS) contendo PQs foram obtidos com diâmetro hidrodinâmico entre 100-220 nm. A formulação preparada com DSPE-Peg apresentou maior intensidade de emissão no visível quando comparadas com as NLS. O estudo de estabilidade realizado com as NLS luminescentes em diferentes meios (água, PBS, PBS com Mg e Ca, RPMI com soro à 10%) à 37°C durante 3 horas, mostrou que o tamanho delas não variou bruscamente no tempo analisado. Nesse estudo o tamanho máximo

encontrado foi de 300 nm, mostrando que na presença de proteínas, elas não formam grandes agregados que podem favorecer a fagocitose pelo sistema mononuclear. Foram utilizados três métodos para realizar o estudo de internalização celular. O estudo da associação de fluorescência mostrou aumento da intensidade de emissão no visível de células de macrófagos J774 tratadas com 2 mg/mL de NLS luminescente durante 50 min, comparado com as células sem tratamento. Este resultado sugere internalização parcial das NLS nos macrófagos. A vídeo-microscopia e a microscopia de fluorescência não tiveram su-

cesso para realizar este estudo, uma vez que as condições experimentais utilizadas não puderam superar o efeito de auto-fluorescência das células. Para concluir, a síntese de PQs à base de ZnO pelo processo sol-gel possibilitou estudar as estruturas e propriedades luminescentes destes, permitindo otimizar sua síntese para adequá-los para uso como guias luminescentes. Desta forma,  $Zn_{0.8}Mg_{0.2}O$  com alto rendimento quântico foi incorporado em nanocarreadores lipídicos e sua aplicação como guia luminescente foi evidenciada através do teste de associação de fluorescência.

## *Acknowledgements*

Firstly, I thank **God** for always guide me.

**Bruno** by his company, motivation, knowledge, help, good humor, love and affection.

To my family, especially my parents, **Cida** and **Oswaldo**, my sisters **Juliana** and **Mariele**, my brother in law **Eduardo** and my nieces **Sarah**, **Luana** and **Rafaela** by their love and encouragement.

I thank my supervisors Prof. Dr. **Leila Aparecida ChiavacciFavorin** and Dr. **Claudie Bourgaux** and my co-advisor Dr. **Renata C. K. Kaminski** for their dedication, supervision, motivation, and patience.

My friends of **CMAF laboratory** **Marina**, **BrunaLallo**, **Bruna Chiari**, **Neima**, **Gabriela**, **João**, **Mariluci**, **Flavia**, **Aline** and **Natalia** for their help, support, and also **Mariana Sato**, **Jéssica** and **Alice**.

The friendships of **Institut Galien** **Andreza**, **Any**, **André**, **Júnior**, **Thais**, **Benedict**, **Cristina**, **Leila**, **Chau**, **Boris**, **Frank**, **Elodie**, **Sarah** and also Dr. **François-XavierLegrand**, Dr. **Vincent Faivre**, **Jean-Jacques**, **David**, Dr. **Angéline Angelova**, **Fany**, Dr. **Gillian Barratt**, **Claire**, **Alice**, **Fatima**, Dr. **Christine Vauthier**, Dr. **Didier Desmaele** and Dr. **Sylviane Lesieur**.

The Brazilian friends that I met in France **Sara Bachner**, **Rodrigo** (Dido), **Dani**, **Kellen** and all those that were visit me when I was in Paris **Má**, **Sarah**, **Cidinha**, **Patty**, **Marina**, **Roberto**, **Milena**, **Tia Rô**, **Carol**, **André** (Presidente), Mrs **Sonia**, Mr **Antônio**, **Gisele**, **Cavalim**, **Tia Eliana**, **Tia Eloísa**, **Daniel** and those that we met by chance **Marcel**, **Natália**, **Milana** and **Gledson**.

The Brazilian neighbors of 1, Rue Gustave Geffroy, **Sarah** and **Helena**, lovely women.

The **Chemical Institute** of UNESP/Araraquara, especially teachers Dr. **Celso V. Santilli**, Dr. **Sandra Helena Pulcineli**, Dr. **Peter Hammer**, the colleagues **Nalva**, **Aline**, **Bianca**, **Marlon**, **Rodrigo**, **Rodolfo** and specially **Marina** and **Amélie** for their supporting during HRTEM and EXAFS understandings, respectively, and the laboratory technicians **Sérgio**, **Rafael** and **Ricardo**.

The synchrotron **SOLEIL** for providing beamtime at the SAMBA beamline (project number: 20131299), Dr. **Valérie Briois** for her support during EXAFS experiments and all her knowledge, discussions, and help during my thesis; SWING beamline (project number: 20131299) **J. Perez**, **Y. Liatimi** and **Pierre Roblin** for their support during SAXS experiments; **Stéphanie Blanchandin** and **Karine Chaouchi** for WAXS measurements and their kindly support at the Chemistry Laboratory of SOLEIL.

The **LNLS** (project number: 14321) for SAXS measurements, Dr. **Florian Meneau** for his support during SAXS understanding, motivation and friendship, **LNNano** for HRTEM measurements.

The **Service of electronic microscopy** of the University Pierre et Marie Curie for HRTEM measurements.

The secretaries of **Post-Graduation Technique Section of Faculty of Pharmaceutical Sciences**, **Claudia**, **Daniela**, **Joyce**, **Flávia** and the secretary of **Doctoral School “Innovation thérapeutique du fondamental à l'appliqué”** Mme **Lucie Landry**.

**FAPESP** (Process number: 2012/07570-4 and BEPE process number: 2015/01198-4) and **PADC/FCF-UNESP** for the financial support.

My thesis was conducted at the Institut Galien of University Paris - Sud during one year supported by the International Cooperation Program **CAPES/COFECUB** (ME 767-13), financed by CAPES – Brazilian Federal Agency for Support and Evaluation of Graduate Education within the Ministry of Education of Brazil.

To all those who directly or indirectly contributed to the realization of this thesis, thank you very much.

## List of Figures

- Figure I.1. Schematic structures of the nanocarriers: (a) Polymeric nanoparticles, (b) Liposomes, (c) Lipid nanoparticles and nanoemulsions, (d) Micelles, (e) Cyclodextrins, (f) Dendrimers, (g) Carbon nanotubes, (h) Gold nanoparticles. **Erro! Indicador não definido.**
- Figure I.2. Illustration of the EPR effect of drug-loaded nanocarriers (macromolecule) in a malignant tissue. .... **Erro! Indicador não definido.**
- Figure I.3. Absorption coefficient of oxyhemoglobin, hemoglobin and water from 400 to 1000 nm. The inset shows the lowest absorption coefficient in the NIR region around 650–900 nm. .... **Erro! Indicador não definido.**
- Figure I.4. Schematic representation of lipid-based nanocarriers. **Erro! Indicador não definido.**
- Figure I.5. Schematic structures of the three generations of liposomes. **Erro! Indicador não definido.**
- Figure I.6. Schematic size-dependent luminescence properties of QDs: correlation between the electronic structure of QDS and the QD radius which leads to the blue shift of the emitted ration due to quantum confinement as the QD size decreases. **Erro! Indicador não definido.**
- Figure I.7. Solutions of CdSe/CdS core-shell QDs with different size and shell thickness under normal indoor light (no UV radiation). .... **Erro! Indicador não definido.**
- Figure I.8. Schematic structure of the core-shell quantum dot capped by amphiphilic molecules. .... **Erro! Indicador não definido.**
- Figure I.9. A mouse under UV light ( $\lambda_{exc} = 330$  nm) (A) after 5 min after intradermal injection of green QDS, and (B) 60 min after intradermal injection of green and yellow QDS. .... **Erro! Indicador não definido.**
- Figure I. 10. Schematical structure of wurtzite ZnO, where Zn is the grey ball and O is the red ball, both Zn and O ions fourfold coordinated. .... **Erro! Indicador não definido.**
- Figure I.11. Suggested mechanisms involved in the ZnO photoluminescent processes: (a) typical exciton emission (UV emission), (b) recombination of a shallowly trapped electron with a deeply trapped hole, and (c) recombination of a shallowly trapped hole with a deeply trapped electron (visible emission). In the maps VB and CB are the valence band and the conductance band, respectively. .... **Erro! Indicador não definido.**

Figure I.12. PL spectra of the ZnO nanoparticles synthesized at (a) 50, (b) 100, (c) 150 and (d) 200 °C, measured at room temperature with excitation wavelength 280 nm..... **Erro! Indicador não definido.**

**Indicador não definido.**

Figure I.13. Schematic diagram of Co-doped ZnO QDs structure.**Erro! Indicador não definido.**

Figure II.1. Molecule of (a) DPPC, (b) DSPE-Peg 2000, and (c) oleic acid.**Erro! Indicador não definido.**

Figure II.2. Experimental setup for ZnAc precursor preparation.**Erro! Indicador não definido.**

Figure II.3. The Bragg description of diffraction in terms of the reflection of a plane wave (wavelength  $\lambda$ ) incident at an angle  $\theta$  to atomic planes of spacing  $d$ .**Erro! Indicador não definido.**

Figure II.4. (a) Schematic SAXS setup and (b) X-ray beam paths from the source to the detector, both elements located far away from the sample.**Erro! Indicador não definido.**

Figure II.5. Schematical setup used at SWING beamline. .... **Erro! Indicador não definido.**

Figure II.6. Illustration of a typical X-ray absorption,  $\mu_x$  versus  $E$ , for PD and a brief explanation of the principle of X-ray absorption spectroscopy both in terms of XANES and EXAFS spectroscopy..... **Erro! Indicador não definido.**

Figure II.7. ZnO QDs UV absorption spectra appointing  $\lambda$  determined by Nedeljkovic.. **Erro! Indicador não definido.**

Figure II.8. Schematic figure of the plate used to perform the determination of the fluorescence association by fluorescence spectroscopy..... **Erro! Indicador não definido.**

Figure II. 9. Schematic figure of the plate used to perform the cell treatment with luminescent nanoparticles for further observation by fluorescence microscope.**Erro! Indicador não definido.**

Figure III.1. (a)XRD profiles of ZnO and ZnS standards, ZnO and ZnS QDs, and ZnO/ZnS core-shell QDs with different concentration of the sulphur source. (b)Marked lines indicating the hexagonal wurtzite phase (black) and cubic zinc blende phase (red) are shown. Zoom of the peaks (111), (100), (002) and (101) in the  $2\theta$  ranging from 23 to 40 ° of the ZnO QDs, ZnS QDs, SUSP\_TAA5mM and PREC\_TAA5mM.**Erro! Indicador não definido.**

Figure III.2. (a) XANES spectra and (b) Fourier Transforms of EXAFS spectra recorded for the different samples and ZnO and ZnS standard references. **Erro! Indicador não definido.**

Figure III.3. HRTEM image of (a) SUSP\_TAA5mM and (b) a zoom of the sample SUSP\_TAA5mM which shows the interplanar spacing of ZNO and ZNS phases. .... **Erro! Indicador não definido.**

Figure III.4. UV-vis spectra of (a) ZnO QDs, ZnS QDs and the mixture of ZnO and ZnS QDs and (b) ethanolic solution of TAA. .... **Erro! Indicador não definido.**

Figure III.5. Selected UV-vis spectra measured at the indicated reaction time (min) of the reactions using the Route 1 on the left ((a) SUSP\_TAA1.5mM, (b) SUSP\_TAA5mM and (c) SUSP\_TAA50mM) and the Route 2 on the right ((d) PREC\_TAA1.5mM, (e) PREC\_TAA5mM and (f) PREC\_TAA50mM). .... **Erro! Indicador não definido.**

Figure III.6. (a) Zoom of selected UV-vis spectra measured at the indicated reaction time (min) in the region of the excitonic peak of ZnO QDs (330 to 360 nm) of the SUSP\_TAA50mM reaction, and (b) UV-vis spectrum of SUSP\_TAA50mM reaction product washed and re-suspended in etanol. .... **Erro! Indicador não definido.**

Figure III.7. Time evolution of the pH during the reactions using Route 1 (a) and Route 2 (b). .... **Erro! Indicador não definido.**

Figure III.8. Selected in situ SAXS profiles measured at the indicated reaction time (min) of ZnO QDs (a) and the reactions using the Route 1 (b, c and d) and the Route 2 (e, f and g). .... **Erro! Indicador não definido.**

Figure III.9. Time evolution of the Rg (nm) during 40 min of the reactions (except for the reaction SUSP\_TAA5mM which presented the plateau in the Guinier region up to 20 min). .... **Erro! Indicador não definido.**

Figure III.10. PL spectra of the ZnO QDs, samples prepared using the Route 1 (SUSP\_TAA1.5mM, SUSP\_TAA5mM and SUSP\_TAA50mM) and the Route 2 (PREC\_TAA1.5mM, PREC\_TAA5mM and PREC\_TAA50mM) excited at 353 nm. .... **Erro! Indicador não definido.**

Figure III.11. Time evolution of (a) the pH, ZnO and TAA UV-vis absorbance intensity of the SUSP\_TAA50mM and (b) the pH and TAA UV-vis absorbance intensity of the PREC\_TAA50mM. .... **Erro! Indicador não definido.**

Figure IV.1. (a) XRD profiles of the ZnO standard and nanocrystals from the reactions with 0,

2.5, 5, 10 and 20 % of Mg precursor concentration, indicating the hexagonal wurtzite phase and (b) zoom of the peak (100) in the  $2\theta$  ranging from 30 to 34. **Erro! Indicador não definido.**

Figure IV.2. HRTEM images of undoped ZnO QDs (a) and  $Zn_{0.8}Mg_{0.2}O$  QDs (b). ..... **Erro! Indicador não definido.**

Figure IV.3. Three-dimensional stacked log-log plots of the SAXS curves as a function of time recorded in situ during the formation of ZnO QDs (a) and selected in situ SAXS profiles measured at the indicated reaction time (min) (b). **Erro! Indicador não definido.**

Figure IV.4. Three-dimensional stacked log-log plots of the SAXS curves as a function of time recorded in situ during the formation of  $Zn_{0.8}Mg_{0.2}O$  QDs (a) and selected in situ SAXS profiles measured at the indicated reaction time (min) (b). **Erro! Indicador não definido.**

Figure IV. 5. Comparison of the time evolution of the radius of gyration ( $R_g$ ) determined by the Guinier region and the radius of Sphere ( $R$ ) determined by the sphere model of (a) ZnO QDS and (b)  $Zn_{0.8}Mg_{0.2}O$  QDs. .... **Erro! Indicador não definido.**

Figure IV.6. Raman spectra of ZnO standard, ZnO QDs,  $Zn_{0.8}Mg_{0.2}O$  QDs, OA, OA-ZnO QDs and OA-  $Zn_{0.8}Mg_{0.2}O$  QDs with indications of the principal vibrations (a) from 200 to  $800\text{ cm}^{-1}$  and (b) from  $800$  to  $1800\text{ cm}^{-1}$ . .... **Erro! Indicador não definido.**

Figure IV.7. Absorption spectra of the undoped and 2.5, 5, 10 and 20% Mg doped ZnO colloidal suspensions. .... **Erro! Indicador não definido.**

Figure IV. 8. PLE and PL spectra of the undoped and 2.5, 5, 10 and 20 mol% Mg doped ZnO colloidal suspensions. The inset shows the photography of the undoped (right) and  $Zn_{0.8}Mg_{0.2}O$  (left) colloidal suspensions under UV lamp ( $\lambda_{exc} = 365\text{ nm}$ ). ..... **Erro! Indicador não definido.**

Figure IV.9. PL spectra of the OA-ZnO QDs and OA-  $Zn_{0.8}Mg_{0.2}O$  QDs dispersed in chloroform. The insets show the photographs of each sample under UV lamp ( $\lambda_{exc} = 365\text{ NM}$ ). .... **Erro! Indicador não definido.**

Figure V.1. Principal nanocarriers endocytic pathways in mammalian cells: (a) Phagocytosis, an actin-based mechanism, closely associated with opsonization; (b) Clathrin-mediated endocytosis, associated with the formation of a clathrin lattice; (c) Caveolae-mediate endocytosis, typical flask-shaped invaginations of the membrane coated with caveolin dimers; (d) Macropinocytosis, also an actin-based pathway, less selective than



phagocytosis; (e) Other endocytosis pathways, independent of both clathrin and caveolae-mediation..... **Erro! Indicador não definido.**

Figure V.2. SAXS patterns of DPPC based liposomes formulations collected at 30°C. ... **Erro! Indicador não definido.**

Figure V.3. SAXS patterns of DPPC based liposomes formulations collected at 50°C. ... **Erro! Indicador não definido.**

Figure V.4. Cryo-TEM images of formulation similar to D5 in a large excess of water, after extrusion..... **Erro! Indicador não definido.**

Figure V.5. SAXS patterns of DSPE-Peg based formulations collected at 30 °C. .... **Erro! Indicador não definido.**

Figure V.6. SAXS patterns of DSPE-Peg/DPPC based formulations collected at (a) 30°C (continuous lines) and (b) 50°C (dotted lines). .... **Erro! Indicador não definido.**

Figure V. 7. Cryo-TEM images of formulations DPeg6. .... **Erro! Indicador não definido.**

Figure V.8. Photos of (a)the dried film, (b)the hydrated film under visible light and (c) under UV lamp ( $\lambda_{exc} = 356\text{nm}$ ) of the DPeg6 formulation..... **Erro! Indicador não definido.**

Figure V.9. Cryo-TEM images of formulation (a) G12, and (b) THF.**Erro! Indicador não definido.**

Figure V.10. Photos of the formulations G1-G9 (from left to right) under UV lamp ( $\lambda_{exc} = 356\text{nm}$ ). .... **Erro! Indicador não definido.**

Figure V.11. Absorption spectra of the diluted formulations G4, G8, and DPeg6. .... **Erro! Indicador não definido.**

Figure V.12. (a) PLE and (b) PL spectra of the formulations G4, G8 and DPeg6..... **Erro! Indicador não definido.**

Figure V.13. Absorption spectra of the water and cells suspension.**Erro! Indicador não definido.**

Figure V.14. PL spectra of (a) cells suspension excited at 270, 340, 350, and 365 nm and (b) a zoom in the PL spectra excited at 340, 350, and 365 nm... **Erro! Indicador não definido.**

Figure V.15. Evolution of the mean size of the formulation G4 in different media during the time..... **Erro! Indicador não definido.**

Figure V.16. PL spectra of lysed cells without treatment, cells treated with 1 and 2 mg/mL of G4 nanoparticles excited at (a) 340 nm and (b) 365 nm. .... **Erro! Indicador não definido.**

Figure VI.1. Schematical final products obtained in the reactions starting from ZnO colloidal

suspensions (Route 1) and ZnAc precursor (Route 2) using three TAA concentrations (1.5, 5 and 50mM).....	57
Figure VI.2. Schematical structures of ZnO and Zn <sub>0.8</sub> Mg <sub>0.2</sub> O QDs with and without OA capping, their photographs and respective QY..	58
Figure VI.3. Photographs of QDs loaded liposomes, a DSPE-Peg based formulation and an example of SLN (from left to right, respectively) under UV lamp.....	59

## List of tables

Table III. 1. EXAFS structural parameters for the first Zinc coordination sphere of ZnO, for the first Zinc coordination sphere of ZnS, and the percentages of ZnO and ZnS deduced from the Linear Combination Fittings (LCF) of XANES spectra. <b>Erro! Indicador não definido.</b>
Table III.2. Initial (time = 1 min) and Final (time = 40 min) ZnO QDs Radius (nm) deduced

from UV-vis spectra using Brus Equation, and Initial (time = 1 min) and Final (time = 40 min)  $R_g$  (nm) deduced from SAXS curves using Guinier Equation. **Erro! Indicador não definido.**

Table IV. 1. Amount of Mg incorporated into ZnO QDs obtained by ICP, Crystallite size deduced from X-ray diffraction peaks using the Debye-Scherrer relation, Bandgap measured using UV-vis absorption, Wavelength of the PLE peak maximum, Wavelength of the PL emission peak maximum, Quantum Yield of each sample. **Erro! Indicador não definido.**

Table IV.2. Variables  $N$  (particle number density),  $s$  (polydispersity), and  $X_0$  (mean radius) used to fit the ZnO and  $Zn_{0.8}Mg_{0.2}O$  SAXS curves and the values of  $I(0)$  obtained by Guinier equation ..... **Erro! Indicador não definido.**

Table IV. 3. Raman shift ( $cm^{-1}$ ) and assignment of the main vibrations observed in the following samples: ZnO standard, ZnO QDS,  $Zn_{0.8}Mg_{0.2}O$  QDS, OA, OA-ZnO QDS and  $OA-Zn_{0.8}Mg_{0.2}O$  QDs. Raman shifts are compared with values from References (TANDON et al., 2000; KOLEVA e STOILOVA, 2002; CUSCÓ et al., 2007; DE GELDER et al., 2007). ..... **Erro! Indicador não definido.**

Table IV.4. Quantum Yield (QY) of the ZnO and  $Zn_{0.8}Mg_{0.2}O$  QDs capped with oleic acid (OA). ..... **Erro! Indicador não definido.**

Table V.1.  $OA-Zn_{0.8}Mg_{0.2}O$  QDs, DPPC and water quantities used in the liposomes formulations, QD/DPPC ratio (mg/mg) and  $d$ -spacing at 30 and 50 °C. **Erro! Indicador não definido.**

Table V.2.  $OA-Zn_{0.8}Mg_{0.2}O$  QDs, DSPE-Peg and water quantities used in the formulations, QD/DSPE-Peg ratio (mg/mg) and  $d$ -spacing at 10, 30 and 50 °C. **Erro! Indicador não definido.**

Table V.3.  $OA-Zn_{0.8}Mg_{0.2}O$  QDs, DPPC, DSPE-Peg and water quantities used in the formulations, QD/lipids ratio (mg/mg) and  $d$ -spacing at 30 and 50 °C. **Erro! Indicador não definido.**

Table V.4.  $Zn_{0.8}Mg_{0.2}O$  QDs and Gelucire concentrations, ratio of  $Zn_{0.8}Mg_{0.2}O$  QDs:Gelucire 50/13® and ethanol:water used. .... **Erro! Indicador não definido.**

## List of abbreviations

Ab: antibody

AET: aminoethanethiol-HCl

AFM : atomic force microscopy

CMC: critical micellar concentration

Cryo-TEM: cryogenic transmission electron microscopy

CT :Computed Tomography

DPPC: 1,2-dipalmitoyl-sn-glycero-3-phosphocholine

DSPE-Peg:1,2-distearoyl-sn-glycero-3-phosphoethanolamine-N-[amino(polyethylene glycol)-2000] ammonium salt

EGFR: epidermal growth factor receptor

EPR: enhanced permeation and retention

EXAFS: extended X-ray absorption fine structure

FT: Fourier transform

FWHM: full width at half maximum

GUV: giant unilamellar vesicles

HA: hyaluronic acid

HepG2: human liver carcinoma cells

HDS: hydroxy double salts

HRTEM: High Resolution Transmission Electron Microscopy

ICP – MS: Inductively Coupled Plasma Mass Spectrometry

J774: murine phagocytic macrophage-like cell line

LCF: Linear Combination Fittings

LNC: lipid nanocapsules

LUV: large unilamellar vesicles

MHDA: 16-mercaptohexadecanoic acid

MLV: multilamellar vesicles

MOF: metal organic frameworks

MPS: mononuclear phagocyte system

MRI: magnetic resonance imaging

MUA: 11-mercaptoundecanoic acid

NCs: nanocarriers

NIR: near-infrared

NPs: Nanoparticles

OA: oleic acid

OA-ZnO QDs: ZnO quantum dots with oleic acid as surface modifier

OA-  $Zn_{1-x}Mg_xO$  QDs: Mg-doped ZnO quantum dots with oleic acid as surface modifier

PBS: Phosphate-buffered saline

PEG: polyethylene glycol

PL: Photoluminescence

PLE : excitation photoluminescence

PREC: precursor

QDs: quantum dots

QD-LN: SLNs containing  $Zn_{0.8}Mg_{0.2}O$  QDs

QELS: Quasi Elastic Light Scattering

QY: Quantum Yield

RES: reticuloendothelial system

RF: red phenol

Rg: radius of gyration

ROS: reactive oxygen species

RPMI: Roswell Park Memorial Institute, medium of cell culture

SAXS: Small Angle X-Ray Scattering

SLN: solid lipid nanoparticles

SR: synchrotron radiation

SUSP: Suspension

SUV: Small unilamellar vesicles

TAA: Thioacetamide

THF: tetrahydrofuran

UV-vis: ultraviolet-visible

XANES: X-ray absorption near-edge structure

XAS: X-Ray Absorption Spectroscopy

XDR: X-Ray Diffraction

XES: X-ray emission spectroscopy

XPS: X-ray Photoelectron Spectroscopy

ZnO Susp: ZnO colloidal suspensions

$Zn_{1-x}Mg_xO$  QDs: Mg-doped ZnO quantum dots with x amount of Mg

# CONTENT

INTRODUCTION .....	23
--------------------	----

## CHAPTER I - Bibliography

I.1. Nanomedicine as a theranostic system.....	27
I.2. Lipid-based nanocarriers .....	31
I.2.1. Liposomes .....	32
I.2.2. Micelles .....	34
I.2.3. Solid lipid nanoparticles (SLN) .....	35
I.2.4. Lipid nanocapsules (LNC) .....	35
I.3. Quantum Dots for optical imaging.....	36
I.3.1. Core-shell QDs.....	37
I.3.2. Surface-modification of QDs with organic molecules.....	39
I.3.3. In vitro imaging using QDs.....	39
I.3.4. In vivo imaging using QDs .....	40
I.3.5. ZnO QDs .....	41
I.3.5.1. Sol-gel synthesis.....	41
I.3.5.2. Photoluminescence properties.....	43
I.3.6. Doped ZnO QDs .....	46
I.3.7. Toxicity of quantum dots .....	47
I.4. References .....	50

## CHAPTER II - Materials and methods

II.1. Materials .....	65
II.2. Synthesis .....	66
II.2.1. ZnO QDs.....	66
II.2.2. ZnS QDs .....	67
II.2.3. ZnO/ZnS core-shell QDs and ZnO and ZnS QDs mixtures .....	67
II.2.4. $Zn_{1-x}Mg_xO$ QDs .....	67
II.2.5. Powder obtainment .....	68

II.2.6.Oleic acid-surface modified QDs: OA-ZnO QDs and OA-Zn <sub>0.8</sub> Mg <sub>0.2</sub> O QDs.....	68
II.3.QDs incorporation into lipid-based nanocarriers.....	68
II.3.1.Preparation of DPPC and DSPE-Peg 2000 –based formulations .....	68
II.3.2.Preparation of Solid Lipid Nanoparticles (SLN) containing QDs.....	68
II.4.Characterizations.....	69
II.4.1.X-ray diffraction (XRD) .....	69
II.4.2.Small-Angle X-ray Scattering (SAXS).....	70
II.4.3.X-ray Absorption Spectroscopy (XAS).....	73
II.4.4.Inductively Coupled Plasma Mass Spectrometry (ICP-MS) .....	76
II.4.5.Raman Spectroscopy.....	76
II.4.6. High Resolution Transmission Electron Microscopy (HRTEM) .....	76
II.4.7.UV-vis Spectroscopy .....	76
II.4.8.Photoluminescence Spectroscopy (PL).....	78
II.4.9.Cryo microscopy.....	79
II.4.10.Study of the Stability of SLN containing QDs .....	79
II.4.11.Cell culture and preparation.....	79
II.4.12.Internalization Study.....	79
II.4.12.1.Determination of the fluorescence of cells .....	80
II.4.12.2.Live-cell imaging using video-microscopy .....	80
II.4.12.3.Fluorescence microscopy.....	81
II.4.References.....	83

### CHAPTER III – Study of ZnO/ZnS core-shell QDs formation by sol-gel process

III.1. Introduction .....	87
III.2. Results .....	89
III.2.1.X-ray diffraction (XRD).....	89
III.2.2.X-ray Absorption Spectroscopy (XAS).....	90
III.2.3.High Resolution Transmission electron microscopy.....	94
III.2.4.In situ UV-vis spectroscopy .....	95
III.2.5.pH evolution .....	99
III.2.6.In situ small Angle X-ray Scattering .....	101
III.2.7.Photoluminescence .....	104

III.3.Discussions .....	105
III.4.Conclusions .....	109
III.5.References .....	110

#### CHAPTER IV – Surface modified Mg-doped ZnO QDs for biological imaging

IV.1. Introduction .....	115
IV.2. Results .....	116
IV.2.1.Inductively Coupled Plasma Mass Spectrometry (ICP-MS).....	117
IV.2.2.X-ray powder diffraction (XRD).....	117
IV.2.3.High Resolution Transmission electron microscopy (HRTEM).....	119
IV.2.4.Small-Angle X-ray Scattering (SAXS) .....	119
IV.2.5.Raman Spectroscopy .....	123
IV.2.6.UV-vis and Photoluminescence Spectroscopy (PL) .....	125
IV.3. Discussions .....	128
IV.4. Conclusions .....	131
IV.5. References .....	132

#### CHAPTER V – Mg-doped ZnO QDs incorporated in lipid based nanocarriers and their application in cell internalization investigations

V.1. Introduction .....	137
V.2. Results and discussions .....	138
V.2.1. DPPC-based formulations .....	138
V.2.2. DSPE-Peg based formulations.....	142
V.2.3.Solid lipid nanoparticles .....	145
V.2.4. PL studies .....	148
V.2.5.Nanoparticle stability studies.....	151
V.2.6. Cell internalization studies .....	152
V.3. Conclusions .....	154
V.4.References.....	155



## CHAPTER VI – Final conclusions and Perspectives

VI.1. Final conclusions .....	158
VI.2. Perspectives .....	161
ANNEXES .....	164

# INTRODUCTION

## **Introduction**

The use of nanotechnology in the biomedical field is increasing due to the advantages of drug nanocarriers. For instance, nanoparticles loaded with drugs may improve the solubility and bioavailability of poorly soluble drugs, protect them from degradation, cross biological barriers, decrease drug toxicity against healthy cells by delivering the drug in target tissues. The drug loading capacity, biodistribution, pharmacokinetics and toxicity of nanoparticles depend on their composition, size, structure and surface properties. For example, nanoparticle surface modification by hydrophilic polymers or specific ligands has been explored to promote longer circulation time or to guide them to target tissue. Lipid based nanocarriers, such as liposomes, phospholipid micelles and solid lipid nanoparticles, are widely investigated due to their biocompatibility and biodegradability.

Theranostic devices arise from the combination of therapeutic and imaging agents in a unique nanoparticle, in order to follow the nanoparticle biodistribution and to evaluate the disease evolution.

Numerous imaging agents can be used in theranostic nanoparticles, depending on the type of image: radionuclides for nuclear imaging, heavy elements for computed tomography, superparamagnetic metal oxides for magnetic resonance imaging and fluorescent dyes or quantum dots (QDs) for optical imaging. QDs have gained place because they present original properties, such as a large absorption spectrum, a narrow emission band and bright signal. Cadmium (Cd) based QDs were the first and most explored QDs for bioimaging application; however, they present high toxicity as well as other heavy metal based QDs. To minimize the toxic effects, core-shell QDs and surface capped QDs were developed in order to prevent the release of heavy ions in the biological media. Moreover, coating QDs with a higher band gap semiconductor can eliminate surface defects, which minimizes the photoblinking effect, and QDs surface modification with organic molecules can provide colloidal stability in aqueous media or non-polar solvents. Nevertheless, nontoxic QDs, such as ZnO or ZnS QDs, began to be used due to their biocompatibility and promising photoluminescent properties.

The photoluminescence of ZnO QDs is directly related to their size and surface defects. Because of these important characteristics, the synthesis route strongly interferes with the final properties of the material. Since 1980, researchers have studied the quantum confinement and luminescent properties of ZnO QDs synthesized using the sol-gel route,

which allows obtaining nanoparticles with size varying from 2 to 6 nm, displaying surface defects such as oxygen vacancies. However, the visible luminescence of ZnO QDs vanishes in the presence of water because they tend to aggregate, precipitate and their luminescent centers are destroyed. For this reason, the challenge is to keep their visible photoluminescence emission in biological media to allow their use in bioimaging.

The aim of this work was to develop ZnO based QDs with strong visible emission, stable in biological media or organic solvent that allow their later incorporation in lipid based nanocarriers, in order to achieve theranostic devices.

In the first part (Chapter III), ZnO/ZnS core-shell QDs were developed using a low-temperature sol-gel route. The formation of ZnS shell around the ZnO core could provide UV photoluminescence stability and prevent photoblinking and photobleaching undesirable effects. Numerous techniques, such as Small Angle X-Ray Scattering (SAXS), UV-Vis Spectroscopy, pH, X-Ray Absorption (XAS), High Resolution Transmission Electron Microscopy (HRTEM), X-Ray Diffraction (XRD) were used to monitor the reactions and characterize the materials obtained. When characterized by Photoluminescence Spectroscopy, ZnO/ZnS core-shell QDs did not present an increase in the emission intensity in the visible range.

Because of ZnO/ZnS structures did not demonstrate desirable optical properties, the optimization of ZnO QDs for imaging was performed differently. Chapter IV described ZnO QDs doped with Mg<sup>2+</sup> ions with enhanced luminescence emission. Specifically, we have shown that the maximum quantum yield (QY = 64%) for Mg precursor concentration of 20 mol% was six times higher than for undoped ZnO QDs (QY = 10%). Mg-doped ZnO QDs were characterized in order to establish a relationship between the composition and structure of the QDs and their luminescent properties.

The surface modification of the QDs was then performed using oleic acid (OA) to hinder their aggregation and to provide them colloidal stability in non-polar environment. Still in the Chapter IV, we could show that Mg-doped ZnO QDs capped by OA formed stable colloidal suspensions in toluene and chloroform, while preserving their photoluminescence with QY around 40 %, promising for bioimaging.

In the Chapter V, the OA surface modified Mg-doped QDs were incorporated in lipid based nanocarriers in order to analyze the nanoparticles structure, stability and luminescence. At low QD concentrations, QDs were embedded within 1,2-dipalmitoyl-sn-glycero-3-phosphocholine (DPPC) bilayers, without perturbing their stacking. 1,2-distearoyl-sn-glycero-

## *Introduction*

---

3-phosphoethanolamine-N-[amino(polyethylene glycol)-2000] ammonium salt(DSPE-Peg) /QDs formulations formed aggregates displaying a close-packed, layered structure, of QDs likely stabilized by a layer of DSPE-Peg. Solid lipid nanoparticles (SLN) loaded with QDs demonstrated good stability in biological media as shown by the absence of large aggregates. Cell internalization studies using luminescent SLN were performed using a macrophage-like cell line. However, cell autofluorescence prevented to unambiguously evidence the internalization of SLN into the cells.

#### **I.4. REFERENCES**

ABDULLAH AL; N. LEE, J.E.; IN, I.; LEE, H.; LEE, K.D.; JEONG, J.H.; PARK; S.Y. Target Delivery and Cell Imaging Using Hyaluronic Acid-Functionalized Graphene Quantum Dots. **Mol Pharm**, v. 10, n. 10, p. 3736-3744, 2013.

ABDULLAH, M.; MORIMOTO, T.; OKUYAMA, K. Generating Blue and Red Luminescence from ZnO/Poly(ethylene glycol) Nanocomposites Prepared Using an In-Situ Method. **Adv Funct Mater**, v. 13, n. 10, p. 800-804, 2003.

ABOULAICH, A., TILMACIU, C.-M., MERLIN, C., MERCIER, C., GUILLOTEAU, H., MEDJAHDI, G., SCHNEIDER, R. Physicochemical properties and cellular toxicity of (poly)aminoalkoxysilanes-functionalized ZnO quantum dots. **Nanotechnology**, v. 23, p. 335101:1-9, 2012.

ACHARYA, S.; SAHOO, S. K. PLGA nanoparticles containing various anticancer agents and tumour delivery by EPR effect. **Adv Drug Deliv Rev**, v. 63, n. 3, p. 170-183, 2011.

ALLEN, T. M.; CULLIS, P. R. Liposomal drug delivery systems: From concept to clinical applications. **Adv Drug Deliv Rev**, v. 65, n. 1, p. 36-48, 2013.

BAHNEMANN, D. W.; KORMANN, C.; HOFFMANN, M. R. Preparation and characterization of quantum size zinc oxide: a detailed spectroscopic study. **J Phys Chem**, v. 91, n. 14, p. 3789-3798, 1987.

BARENHOLZ, Y. Doxil® — The first FDA-approved nano-drug: Lessons learned. **J Control Release**, v. 160, n. 2, p. 117-134, 2012.

BAUM, R. P.; KULKARNI, H. R. THERANOSTICS: From Molecular Imaging Using Ga-68 Labeled Tracers and PET/CT to Personalized Radionuclide Therapy - The Bad Berka Experience. **Theranostics**, v. 2, n. 5, p. 437-447, 2012.

BELOGLAZOVA, N. V.; SHMELIN, P.S.; SPERANSKAYA, E.S.; LUCAS, B.; HELMBRECHT, C.; KNOPP, D.; NIESSNER, R.; DE SAEGER, S.; GORYACHEVA, I.Y. Quantum Dot Loaded Liposomes As Fluorescent Labels for Immunoassay. **Anal Chem**, v. 85, n. 15, p. 7197-7204, 2013.

BHASKAR, S. TIAN, F.; STOEGER, T.; KREYLING, W.; DE LA FUENTE, J. M.; GRAZÚ, V.; BORM, P.; ESTRADA, G.; NTZIACHRISTOS, V.; RAZANSKY, D. Multifunctional Nanocarriers for diagnostics, drug delivery and targeted treatment across blood-brain barrier: perspectives on tracking and neuroimaging. **Part Fibre Toxicol**, v. 7, n. 1, p. 1-25, 2010.

BRIOIS, V. GIORGETTI, C.H.; BAUDELET, F.; BLANCHANDIN, S.; TOKUMOTO, M. S.; PULCINELLI, S. H.; SANTILLI, C. V. Dynamical Study of ZnO Nanocrystal and Zn-HDS Layered Basic Zinc Acetate Formation from Sol–Gel Route. **J Phys Chem CNanomater Interfaces**, v. 111, n. 8, p. 3253-3258, 2007.

BRUNETTI, V. CHIBLI, H.; FIAMMENGO, R.; GALEONE, A.; MALVINDI, M. A.; VECCHIO, G.; CINGOLANI, R.; NADEAU, J. L.; POMPA, P. P. InP/ZnS as a safer alternative to CdSe/ZnS core/shell quantum dots: in vitro and in vivo toxicity assessment. **Nanoscale**, v. 5, n. 1, p. 307-317, 2013.

BRUS, L. E. A simple model for the ionization potential, electron affinity, and aqueous redox potentials of small semiconductor crystallites. **J Chem Phys**, v. 79, n. 11, p. 5566-5571, 1983.

BUONSANTI, R.; MILLIRON, D. J. Chemistry of Doped Colloidal Nanocrystals. **Chem Mater**, v. 25, n. 8, p. 1305-1317, 2013.

CAETANO, B. L. SANTILLI, C. V.; MENEAU, F.; BRIOIS, V.; PULCINELLI, S. H. In Situ and Simultaneous UV–vis/SAXS and UV–vis/XAFS Time-Resolved Monitoring of ZnO Quantum Dots Formation and Growth. **J Phys Chem CNanomater Interfaces**, v. 115, n. 11, p. 4404-4412, 2011.

CAMBLIN, M.; DETAMPEL, P.; KETTIGER, H.; WU, D.; BALASUBRAMANIAN, V.; HUWYLER, J. Polymersomes containing quantum dots for cellular imaging. **Int J Nanomedicine**, v. 9, p. 2287-2298, 2014.

CASSETTE, E.; PONS, T.; BOUET, C.; HELLE, M.; BEZDETAYAYA, L.; MARCHAL, F.; DUBERTRET, B. Cu–In–Se/ZnS Core/Shell Quantum Dots for In vivo Imaging. **Chem Mater**, v. 22, n. 22, p. 6117-6124, 2010.

CHEN, O.; ZHAO, J.; CHAUHAN, V. P.; CUI, J.; WONG, C.; HARRIS, D. K.; WEI, H.; HAN, H. S.; FUKUMURA, D.; JAIN, R. K.; BAWENDI, M. G. Compact high-quality CdSe–CdS core–shell nanocrystals with narrow emission linewidths and suppressed blinking. **Nat Mater**, v. 12, n. 5, p. 445-451, 2013.

CHO, S. J.; MAYSINGER, D.; JAIN, M.; RÖDER, B.; HACKBARTH, S.; WINNIK, F. M. Long-Term Exposure to CdTe Quantum Dots Causes Functional Impairments in Live Cells. **Langmuir**, v. 23, n. 4, p. 1974-1980, 2007.

COHN, A. W.; KITTELSTVED, K. R.; GAMELIN, D. R. Tuning the Potentials of “Extra” Electrons in Colloidal n-Type ZnO Nanocrystals via Mg<sup>2+</sup> Substitution. **J Am Chem Soc**, v. 134, n. 18, p. 7937-7943, 2012.

CONNROT, J. SILVA, J. M., FERNANDES, J. G., SILVA, L. C., GASPAR, R., BROCCINI, S., FLORINDO, H. F., BARATA, T. S. Cancer immunotherapy: nanodelivery approaches for immune cell targeting and tracking. **Front Chem**, v. 2, p. 1-27, 2014.

CONTRERAS, E. Q.; CHO, M.; ZHU, H.; PUPPALA, H. L.; ESCALERA, G.; ZHONG, W.; COLVIN, V.L. Toxicity of Quantum Dots and Cadmium Salt to *Caenorhabditis elegans* after Multigenerational Exposure. **Environ Sci Technol**, v. 47, n. 2, p. 1148-1154, 2013.

DAOU, T. J.; LI, L.; REISS, P.; JOSSERAND, V.; TEXIER, I. Effect of Poly(ethylene glycol) Length on the in Vivo Behavior of Coated Quantum Dots. **Langmuir**, v. 25, n. 5, p. 3040-3044, 2009.

DAZZAZI, A.; COPPEL, Y.; IN, A.; CHASSENIEUX, C.; MASCALCHI, P.; SALOMÉ, L.; BOUHAOUSS, A.; KAHN, M. L.; GAUFFRE, F. Oligomeric and polymeric surfactants for the transfer of luminescent ZnO nanocrystals to water. **J Mater Chem C**, v. 1, n. 11, p. 2158-2165, 2013.

DE JONG, W. H.; BORM, P. J. A. Drug delivery and nanoparticles: Applications and hazards. **Int J Nanomedicine**, v. 3, n. 2, p. 133-149, 2008.

DERFUS, A. M.; CHAN, W. C. W.; BHATIA, S. N. Probing the Cytotoxicity of Semiconductor Quantum Dots. **Nano Lett**, v. 4, n. 1, p. 11-18, 2004.

DESMAËLE, D.; GREF, R.; COUVREUR, P. Squalenoylation: A generic platform for nanoparticulate drug delivery. **J Control Release**, v. 161, n. 2, p. 609-618, 2012.

DONG, Y.; NG, W. K.; SHEN, S.; KIM, S.; TAN, R. B. Solid lipid nanoparticles: Continuous and potential large-scale nanoprecipitation production in static mixers. **Colloids Surf B Biointerfaces**, v. 94, n. 0, p. 68-72, 2012.

DUBERTRET, B.; SKOURIDES, P.; NORRIS, D. J.; NOIREAUX, V.; BRIVANLOU, A. H.; LIBCHABER, A. In Vivo Imaging of Quantum Dots Encapsulated in Phospholipid Micelles. **Science**, v. 298, n. 5599, p. 1759-1762, 2002.

EFROS, A.L. Interband absorption of light in a semiconductor sphere. **Sov Phys Semicond**, v. 16, p. 772-775, 1982.

FATTAL, E.; TSAPIS, N. Nanomedicine technology: current achievements and new trends. **Clin Transl Imaging**, v. 2, n. 1, p. 77-87, 2014.



FERRO-FLORES, G.; OCAMPO-GARCÍA, B. E.; SANTOS-CUEVAS, C. L.; DE MARÍA RAMÍREZ, F.; AZORÍN-VEJA, E. P.; MELÉNDEZ-ALAFORT, L. Theranostic Radiopharmaceuticals Based on Gold Nanoparticles Labeled with <sup>177</sup>Lu and Conjugated to Peptides. **Curr Radiopharm**, v. 8, n. 2, p. 150-159, 2015.

FORTIN-RIPOCHE, J.-P.; MARTINA, M. S.; GAZEAU, F.; MÉNAGER, C.; WILHELM, C.; BACRI, J. C.; LESIEUR, S.; CLÉMENT, O. Magnetic Targeting of Magnetoliposomes to Solid Tumors with MR Imaging Monitoring in Mice: Feasibility. **Radiology**, v. 239, n. 2, p. 415-424, 2006.

FRANK, D.; TYAGI, C.; TOMAR, L.; CHOONARA, Y. E.; DU TOIT, L. C.; KUMAR, P.; PENNY, C.; PILLAY, V. Overview of the role of nanotechnological innovations in the detection and treatment of solid tumors. **Int J Nanomedicine**, v. 9, p. 589-613, 2014.

FU, Y.-S.; DU, X. W.; KULINICH, S. A.; QIU, J. S.; QIN, W. J.; LI, R.; SUN, J.; LIU, J. Stable Aqueous Dispersion of ZnO Quantum Dots with Strong Blue Emission via Simple Solution Route. **J Am Chem Soc**, v. 129, n. 51, p. 16029-16033, 2007.

GABIZON, A.; CATANE, R.; UZIELY, B.; KAUFMAN, B.; SAFRA, T.; COHEN, R.; MARTIN, F.; HUANG, A.; BARENHOLZ, Y. Prolonged Circulation Time and Enhanced Accumulation in Malignant Exudates of Doxorubicin Encapsulated in Polyethylene-glycol Coated Liposomes. **Cancer Res**, v. 54, n. 4, p. 987-992, 1994.

GAO, X.; CUI, Y.; LEVENSON, R. M.; CHUNG, L. W.; NIE, S. In vivo cancer targeting and imaging with semiconductor quantum dots. **Nat Biotech**, v. 22, n. 8, p. 969-976, 2004.

GILL, R.; ZAYATS, M.; WILLNER, I. Semiconductor Quantum Dots for Bioanalysis. **Angew Chem Int Ed Engl**, v. 47, n. 40, p. 7602-7625, 2008.

GOLDMAN, E. R.; BALIGHIAN, E. D.; MATTOUSSI, H.; KUNO, M. K.; MAURO, J. M.; TRAN, P. T.; ANDERSON, G. P. Avidin: A Natural Bridge for Quantum Dot-Antibody Conjugates. **J Am Chem Soc**, v. 124, n. 22, p. 6378-6382, 2002.

GREGORIADIS, G.; RYMAN, B. E. Liposomes as carriers of enzymes or drugs: a new approach to the treatment of storage diseases. **Biochem J**, v. 124, n. 5, p. 58P, 1971.

HAMMAD, T. M.; SALEM, J. K.; HARRISON, R. G.; HEMPELMANN, R.; HEJAZY, N. K. Optical and magnetic properties of Cu-doped ZnO nanoparticles. **J Mater Sci: Mater Electron**, v. 24, n. 8, p. 2846-2852, 2013.

HAN, H.-S.; NIEMEYER, E.; HUANG, Y.; KAMOUN, W. S.; MARTIN, J. D.; BHAUMIK, J.; CHEN, Y.; ROBERGE, S.; CUI, J.; MARTIN, M. R.; FUKUMURA, D.; JAIN, R. K.; BAWENDI, M. G.; DUDA, D.G. Quantum dot/antibody conjugates for in vivo cytometric imaging in mice. **Proc Natl Acad Sci U S A.**, v. 112, n. 5, p. 1350-1355, 2015.

HAN, L.-L.; CUI, L.; WANG, W.-H.; WANG, J.-L.; DU, X.-W. On the origin of blue emission from ZnO quantum dots synthesized by a sol-gel route. **Semicond Sci Technol**, v. 27, n. 6, p. 8, 2012.

HANN, I. M.; PRENTICE, H. G. Lipid-based amphotericin B: a review of the last 10 years of use. **Int J Antimicrob Agents**, v. 17, n. 3, p. 161-169, 2001.

HARDMAN, R. A Toxicologic Review of Quantum Dots: Toxicity Depends on Physicochemical and Environmental Factors. **Environ Health Perspect**, v. 114, n. 2, p. 165-172, 2006.

HEYES, C. D.; KOBITSKI, A. Y.; BREUS, V. V.; NIENHAUS, G. U. Effect of the shell on the blinking statistics of core-shell quantum dots: A single-particle fluorescence study. **Phys. Rev. B**, v. 75, n. 12, p. 125431, 2007.

HINES, M.; GUYOT-SIONNEST, P. Synthesis and Characterization of Strongly Luminescing ZnS-Capped CdSe Nanocrystals. **J Phys Chem**, v. 100, n. 2, p. 468-471, 1996.

HU, Z. RAMÍREZ, D. J. E., CERVERA, B. E. H., OSKAM, G., SEARSON, P. C. Synthesis of ZnO Nanoparticles in 2-Propanol by Reaction with Water. **J Phys Chem B**, v. 109, n. 22, p. 11209-11214, 2005a.

HU, Z., SANTOS, J. F. H., OSKAM, G., SEARSON, P. C. Influence of the reactant concentrations on the synthesis of ZnO nanoparticles. **J Colloid Interface Sci**, v. 288, n. 1, p. 313-316, 2005b.

HU, Z.; OSKAM, G.; SEARSON, P. C. Influence of solvent on the growth of ZnO nanoparticles. **J Colloid Interface Sci**, v. 263, n. 2, p. 454-460, 2003.

HUYNH, N. T.; PASSIRANI, C.; SAULNIER, P.; BENOIT, J. P. Lipid nanocapsules: A new platform for nanomedicine. **Int J Pharm**, v. 379, n. 2, p. 201-209, 2009.

HYUN, B.-R.; CHEN, H.; REY, D. A.; WISE, F. W.; BATT, C. A. Near-Infrared Fluorescence Imaging with Water-Soluble Lead Salt Quantum Dots. **J Phys Chem B**, v. 111, n. 20, p. 5726-5730, 2007.

HYUN, H.; PARK, M. H.; OWENS, E. A.; WADA, H.; HENARY, M.; HANDGRAAF, H. J.; VAHRMEIJER, A. L.; FRANGIONI, J. V.; CHOI, H. S. Structure-inherent targeting of near-infrared fluorophores for parathyroid and thyroid gland imaging. **Nat Med**, v. 21, n. 2, p. 192-197, 2015.

IOANNOU, D.; GRIFFIN, D. K. Nanotechnology and molecular cytogenetics: the future has not yet arrived. **Nano Revs**, v. 1, p. 10.3402/, 2010.

ISNAENI; KIM, K. H.; NGUYEN, D. L.; LIM, H.; NGA, P. T.; CHO, Y.-H. Shell layer dependence of photoblinking in CdSe/ZnSe/ZnS quantum dots. **Appl Phys Lett**, v. 98, n. 1, p. 012109-3, 2011.

JAISWAL, J. K.; MATTOUSSI, H.; MAURO, J. M.; SIMON, S. M. Long-term multiple color imaging of live cells using quantum dot bioconjugates. **Nat Biotech**, v. 21, n. 1, p. 47-51, 2003.

JIA, Z.; MISRA, R. D. K. Tunable ZnO quantum dots for bioimaging: synthesis and photoluminescence. **Mater Technol**, v. 28, n. 4, p. 221-227, 2013.

JIN, S.; HU, Y.; GU, Z.; LIU, L.; WU, H.-C. Application of Quantum Dots in Biological Imaging. **J Nanomater**, v. 2011, p. 13, 2011.

JOSHI, B. P.; WANG, T. D. Exogenous Molecular Probes for Targeted Imaging in Cancer: Focus on Multi-modal Imaging. **Cancers**, v. 2, n. 2, p. 1251-1287, 2010.

KIRCHNER, C.; LIEDL, T.; KUDERA, S.; PELLEGRINO, T.; MUÑOZ JAVIER, A.; GAUB, H. E.; STÖLZLE, S.; FERTIG, N.; PARAK, W. J. Cytotoxicity of Colloidal CdSe and CdSe/ZnS Nanoparticles. **Nano Lett**, v. 5, n. 2, p. 331-338, 2005.

KOBAYASHI, K.; WEI, J.; IIDA, R.; IJIRO, K.; NIKURA, K. Surface engineering of nanoparticles for therapeutic applications. **Polym J**, v. 46, n. 8, p. 460-468, 2014.

KUMAR, S.; SAHARE, P. D. Observation of band gap and surface defects of ZnO nanoparticles synthesized via hydrothermal route at different reaction temperature. **Opt Commun**, v. 285, n. 24, p. 5210-5216, 2012.

KWON, S. R. C. A. G. S. Polymeric Micelles for Drug Delivery. **Curr Pharm Des**, v. 12, n. 36, p. 4669-4684, 2006.

LAMPRECHT, A. Nanomedicines in gastroenterology and hepatology. **Nat Rev Gastroenterol Hepatol**, v. 12, n. 4, p. 195-204, 2015.

LI, L.; DAOU, T. J.; TEXIER, I.; CHI, T. T. K.; LIEM, N. Q.; REISS, P. Highly Luminescent CuInS<sub>2</sub>/ZnS Core/Shell Nanocrystals: Cadmium-Free Quantum Dots for In Vivo Imaging. **Chem Mater**, v. 21, n. 12, p. 2422-2429, 2009.

LI, S., SUN, Z., LI, R., DONG, M., ZHANG, L., QI, W., ZHANG, X., WANG, H. ZnO Nanocomposites Modified by Hydrophobic and Hydrophilic Silanes with Dramatically Enhanced Tunable Fluorescence and Aqueous Ultrastability toward Biological Imaging Applications. **Sci Rep**, v. 5, p. 8475:1-8, 2015.

LIU, Y.; AI, K.; YUAN, Q.; LU, L. Fluorescence-enhanced gadolinium-doped zinc oxide quantum dots for magnetic resonance and fluorescence imaging. **Biomaterials**, v. 32, n. 4, p. 1185-1192, 2011.

LORENZ, C.; EMMERLING, A.; FRICKE, J.; SCHMIDT, T.; HILGENDORF, M.; SPANHEL, L.; MÜLLER, G. Aerogels containing strongly photoluminescing zinc oxide nanocrystals. **J Non Cryst Solids**, v. 238, n. 1-2, p. 1-5, 1998.

LUO, J.; ZHAO, S.; WU, P.; ZHANG, K.; PENG, C.; ZHENG, S. Synthesis and characterization of new Cd-doped ZnO/ZnS core-shell quantum dots with tunable and highly visible photoluminescence. **J Mater Chem C**, v. 3, n. 14, p. 3391-3398, 2015.

MAEDA, H. Tumor-Selective Delivery of Macromolecular Drugs via the EPR Effect: Background and Future Prospects. **Bioconjug Chem**, v. 21, n. 5, p. 797-802, 2010.

MANAIA, E. B., KAMINSKI, R. C. K., CAETANO, B. L., BRIOIS, V., CHIAVACCI, L. A., BOURGAUX, C. Surface modified Mg-doped ZnO QDs for biological imaging. **Eur J Nanomed**, v. 7, p. 109-120, 2015.

MATSUMURA, Y.; MAEDA, H. A New Concept for Macromolecular Therapeutics in Cancer Chemotherapy: Mechanism of Tumor-tropic Accumulation of Proteins and the Antitumor Agent Smancs. **Cancer Res**, v. 46, n. 12 Part 1, p. 6387-6392, 1986.

MOUSSA, H.; MERLIN, C.; DEZANET, C.; BALAN, L.; MEDJAHDI, G.; BEN-ATTIA, M.; SCHNEIDER, R. Trace amounts of Cu<sup>2+</sup> ions influence ROS production and cytotoxicity of ZnO quantum dots. **J Hazard Mater**, v. 304, p. 532-542, 2016.

MOUSSODIA, R.-O., BALAN, L., MERLIN, C., MUSTIN, C., SCHNEIDER, R. Biocompatible and stable ZnO quantum dots generated by functionalization with siloxane-core PAMAM dendrons. **J Mater Chem**, v. 20, p. 1147-1155, 2010.

MULDER, W. J.; KOOLE, R.; BRANDWIJK, R. J.; STORM, G.; CHIN, P. T.; STRIJKERS, G. J.; DE MELLO DONEGÁ, C.; NICOLAY, K.; GRIFFIOEN, A. W. Quantum Dots with a Paramagnetic Coating as a Bimodal Molecular Imaging Probe. **Nano Lett**, v. 6, n. 1, p. 1-6, 2006.

MURA, S.; NICOLAS, J.; COUVREUR, P. Stimuli-responsive nanocarriers for drug delivery. **Nat Mater**, v. 12, n. 11, p. 991-1003, 2013.

MUTHU, M. S.; LEONG, D. T.; MEI, L.; FENG, S. S. Nanotheranostics - Application and Further Development of Nanomedicine Strategies for Advanced Theranostics. **Theranostics**, v. 4, n. 6, p. 660-677, 2014.

NANODIODE, 2015. Disponível em: <http://en.rusnano.com/upload/OldNews/Files/33619/current.gif>. Acesso em: 30 mar.2016.

NICOLAS, J.; MURA, S.; BRAMBILLA, D.; MACKIEWICZ, N.; COUVREUR, P. Design, functionalization strategies and biomedical applications of targeted biodegradable/biocompatible polymer-based nanocarriers for drug delivery. **Chem Soc Rev**, v. 42, n. 3, p. 1147-1235, 2013.

NOEI, H., JIN, L., QIU, H., XU, M., GAO, Y., ZHAO, J., KAUER, M., WÖLL, C., MUHLER, M., WANG, Y. Vibrational spectroscopic studies on pure and metal-covered metal oxide surfaces. **Phys Status Solidi B Basic Solid State Phys**, v. 250, n. 6, p. 1204-1221, 2013.

NORBERG, N. S.; KITTLSTVED, K. R.; AMONETTE, J. E.; KUKKADAPU, R. K.; SCHWARTZ, D. A.; GAMELIN, D. R. Synthesis of Colloidal Mn<sup>2+</sup>:ZnO Quantum Dots and High-TC Ferromagnetic Nanocrystalline Thin Films. **J Am Chem Soc**, v. 126, n. 30, p. 9387-9398, 2004.

OH, E.; LIU, R.; NEL, A.; GEMILL, K. B.; BILAL, M.; COHEN, Y.; MEDINTZ, I. L. Meta-analysis of cellular toxicity for cadmium-containing quantum dots. **Nat Nanotechnol**, v. advance online publication, 2016.

OWENS III, D. E.; PEPPAS, N. A. Opsonization, biodistribution, and pharmacokinetics of polymeric nanoparticles. **Int J Pharm**, v. 307, n. 1, p. 93-102, 2006.

PAN, D.; WANG, Q.; JIANG, S.; JI, X.; AN, L. Synthesis of Extremely Small CdSe and Highly Luminescent CdSe/CdS Core-Shell Nanocrystals via a Novel Two-Phase Thermal Approach. **Adv Mater**, v. 17, n. 2, p. 176-179, 2005.

PAN, J.; WAN, D.; BIAN, Y.; GUO, Y.; JIN, F.; WANG, T.; GONG, T. Reduction of nonspecific binding for cellular imaging using quantum dots conjugated with vitamin E. **AICHE J**, v. 60, n. 5, p. 1591-1597, 2014.

PAN, Z.-Y.; LIANG, J.; ZHENG, Z. Z.; WANG, H. H.; XIONG, H. M. The application of ZnO luminescent nanoparticles in labeling mice. **Contrast Media Mol Imaging**, v. 6, n. 4, p. 328-330, 2011.

PANSARE, V.; HEJAZI, S.; FAENZA, W.; PRUD'HOMME, R. K.. Review of Long-Wavelength Optical and NIR Imaging Materials: Contrast Agents, Fluorophores and Multifunctional Nano Carriers. **Chem Mater.**, v. 24, n. 5, p. 812-827, 2012.

PAPAGIANNAROS, A.; LEVCHENKO, T.; HARTNER, W.; MONGAYT, D.; TORCHILIN, V. Quantum dots encapsulated in phospholipid micelles for imaging and quantification of tumors in the near-infrared region. **Nanomedicine**, v. 5, n. 2, p. 216-224, 2009.

PATTNI, B. S.; CHUPIN, V. V.; TORCHILIN, V. P. New Developments in Liposomal Drug Delivery. **Chemical Reviews**, v. 115, n. 19, p. 10938-10966, 2015.

PELTIER, S.; OGER, J. M.; LAGARCE, F.; COUET, W.; BENOÎT, J. P. Enhanced Oral Paclitaxel Bioavailability After Administration of Paclitaxel-Loaded Lipid Nanocapsules. **Pharm Res**, v. 23, n. 6, p. 1243-1250, 2006.

PENET, M.-F.; MIKHAYLOVA, M.; LI, C.; KRISHNAMACHARY, B.; GLUNDE, K.; PATHAK, A. P.; BHUJWALLA, Z. M.. Applications of molecular MRI and optical imaging in cancer. **Future Med Chem**, v. 2, n. 6, p. 975-988, 2010.

PRADHAN, A. K.; MUNDLE, R. M.; SANTIAGO, K.; SKUZA, J. R.; XIAO, B.; SONG, K. D.; BAHOURA, M.; CHEAITO, R.; HOPKINS, P. E. Extreme tunability in aluminum doped Zinc Oxide plasmonic materials for near-infrared applications. **Sci. Rep.**, v. 4, p. 1-6, 2014.

PURI, A.; LOOMIS, K.; SMITH, B.; LEE, J. H.; YAVLOVICH, A.; HELDMAN, E.; BLUMENTHAL, R.. Lipid-Based Nanoparticles as Pharmaceutical Drug Carriers: From Concepts to Clinic. **Crit Rev Ther Drug Carrier Syst.**, v. 26, n. 6, p. 523-580, 2009.

RABANEL, J. M.; AOUN, V.; ELKIN, I.; MOKHTAR, M.; HILDGEN, P. Drug-Loaded Nanocarriers: Passive Targeting and Crossing of Biological Barriers. **Curr Med Chem**, v. 19, n. 19, p. 3070-3102, 2012.

RATH, T.; KUNERT, B.; RESEL, R.; FRITZ-POPOVSKI, G.; SAF, R.; TRIMMEL, G. Investigation of Primary Crystallite Sizes in Nanocrystalline ZnS Powders: Comparison of Microwave Assisted with Conventional Synthesis Routes. **Inorg Chem**, v. 47, n. 8, p. 3014-3022, 2008.

REISS, P. ZnSe based colloidal nanocrystals: synthesis, shape control, core/shell, alloy and doped systems. **New J Chem**, v. 31, n. 11, p. 1843-1852, 2007.

REISS, P.; PROTÈRE, M.; LI, L. Core/Shell Semiconductor Nanocrystals. **Small**, v. 5, n. 2, p. 154-168, 2009.

SCHMIDT, T.; MÜLLER, G.; SPANHEL, L. Activation of 1.54  $\mu\text{m}$  Er<sup>3+</sup> Fluorescence in Concentrated II-VI Semiconductor Cluster Environments. **Chem Mater**, v. 10, n. 1, p. 65-71, 1998.

SCHWARTZ, D. A.; NORBERG, N. S.; NGUYEN, Q. P.; PARKER, J. M.; GAMELIN, D. R. Magnetic Quantum Dots: Synthesis, Spectroscopy, and Magnetism of Co<sup>2+</sup>- and Ni<sup>2+</sup>-Doped ZnO Nanocrystals. **J Am Chem Soc**, v. 125, n. 43, p. 13205-13218, 2003.

SHARMA, S.; VYAS, R.; SHARMA, N.; SINGH, V.; SINGH, A.; KATARIA, V.; GUPTA, B. K.; VIJAY, Y. K. Highly efficient green light harvesting from Mg doped ZnO nanoparticles: Structural and optical studies. **J Alloys Compd**, v. 552, p. 208-212, 2013.

SIEKMANN, B.; WESTESEN, K. Sub-micron sized parenteral carrier systems based on solid lipid **Pharm. Pharmacol. Lett.**, v. 1, p. 123-126, 1992.

SKANDRANI, N.; BARRAS, A.; LEGRAND, D.; GHARBI, T.; BOULAHDOUR, H.; BOUKHERROUB, R.. Lipid nanocapsules functionalized with polyethyleneimine for plasmid DNA and drug co-delivery and cell imaging. **Nanoscale**, v. 6, n. 13, p. 7379-7390, 2014.

SMITH, A. M.; DUAN, H.; MOHS, A. M.; NIE, S. Bioconjugated quantum dots for in vivo molecular and cellular imaging. **Adv Drug Deliv Rev**, v. 60, n. 11, p. 1226-1240, 2008.

SPANHEL, L.; ANDERSON, M. A. Semiconductor clusters in the sol-gel process: quantized aggregation, gelation, and crystal growth in concentrated zinc oxide colloids. **J Am Chem Soc**, v. 113, n. 8, p. 2826-2833, 1991.

SPELTING, R. A.; PARAK, W. J. Surface modification, functionalization and bioconjugation of colloidal inorganic nanoparticles. **Philos Trans R Soc London, Ser A**, v. 368, n. 1915, p. 1333-1383, 2010.

STOCKHOFE, K.; POSTEMA, J. M.; SCHIEFERSTEIN, H.; ROSS, T. L. Radiolabeling of Nanoparticles and Polymers for PET Imaging. **Pharmaceuticals**, v. 7, n. 4, p. 392–418, 2014.

SU, Y.; HE, Y.; LU, H.; SAI, L.; LI, Q.; LI, W.; WANG, L.; SHEN, P.; HUANG, Q.; FAN, C. The cytotoxicity of cadmium based, aqueous phase – Synthesized, quantum dots and its modulation by surface coating. **Biomaterials**, v. 30, n. 1, p. 19-25, 2009.

SUN, L.-W.; SHI, H.-Q.; LI, W.-N.; XIAO, H.-M.; FU, S.-Y.; CAO, X.-Z.; LI, Z.-X.. Lanthanum-doped ZnO quantum dots with greatly enhanced fluorescent quantum yield. **J Mater Chem**, v. 22, n. 17, p. 8221-8227, 2012.

TANG, J.; KEMP, K. W.; HOOGLAND, S.; JEONG, K. S.; LIU, H.; LEVINA, L.; FURUKAWA, M.; WANG, X.; DEBNATH, R.; CHA, D.; CHOU, K. W.; FISCHER, A.; AMASSIAN, A.; ASBURY, J. B.; SARGENT, E. H. Colloidal-quantum-dot photovoltaics using atomic-ligand passivation. **Nat Mater**, v. 10, n. 10, p. 765-771, 2011.

TERRENO, E.; DASTRÙ, W.; DELLI CASTELLI, D.; GIANOLIO, E.; GENINATTI CRICH, S.; LONGO, D.; AIME, S. Advances in Metal-Based Probes for MR Molecular Imaging Applications. **Curr Med Chem**, v. 17, n. 31, p. 3684-3700, 2010.

TOKUMOTO, M. S., BRIOS, V.; SANTILLI, C. V.; PULCINELLI, S. H. Preparation of ZnO Nanoparticles: Structural Study of the Molecular Precursor. **J Solgel Sci Technol**, v. 26, n. 1-3, p. 547-551, 2003a.

TOKUMOTO, M. S., PULCINELLI, S. H., SANTILLI, C. V. BRIOIS, V. Catalysis and Temperature Dependence on the Formation of ZnO Nanoparticles and of Zinc Acetate Derivatives Prepared by the Sol–Gel Route. **J Phys Chem B**, v. 107, n. 2, p. 568-574, 2003b.

TORCHILIN, V. P. Recent advances with liposomes as pharmaceutical carriers. **Nat Rev Drug Discov**, v. 4, n. 2, p. 145-160, 2005.

VIGLIANTI, B. L.; PONCE, A. M.; MICHELICH, C. R.; YU, D.; ABRAHAM, S. A.; SANDERS, L.; YARMOLENKO, P. S.; SCHROEDER, T.; MACFALL, J. R.; BARBORIAK, D. P.; COLVIN, O. M.; BALLY, M. B.; DEWHIRST, M. Chemodosimetry of in vivo tumor liposomal drug concentration using MRI. **Magn Reson Med**, v. 56, n. 5, p. 1011-1018, 2006.

WANG, X.; REN, X.; KAHEN, K.; HAHN, M. A.; RAJESWARAN, M.; MACCAGNANO-ZACHER, S.; SILCOX, J.; CRAGG, G. E.; EFROS, A. L.; KRAUSS, T. D. Non-blinking semiconductor nanocrystals. **Nature**, v. 459, n. 7247, p. 686-689, 2009.



WANG, Y. S.; THOMAS, P. J.; O'BRIEN, P. Optical properties of ZnO nanocrystals doped with Cd, Mg, Mn, and Fe ions. **J Phys Chem B**, v. 110, n. 43, p. 21412-21415, 2006.

WEI, X.; WANG, W.; CHEN, K. ZnO:Er,Yb,Gd Particles Designed for Magnetic-Fluorescent Imaging and Near-Infrared Light Triggered Photodynamic Therapy. **J Phys Chem C Nanomater Interfaces**, v. 117, n. 45, p. 23716-23729, 2013.

WEISSLEDER, R. A clearer vision for in vivo imaging. **Nat Biotech**, v. 19, n. 4, p. 316-317, 2001.

WEN, C.-J.; ZHANG, L. W.; AL-SUWAYEH, S. A.; YEN, T. C.; FANG, J. Y. Theranostic liposomes loaded with quantum dots and apomorphine for brain targeting and bioimaging. **Int J Nanomedicine**, v. 7, p. 1599-1611, 2012.

WIECINSKI, P. N.; METZ, K. M.; KING HEIDEN, T. C.; LOUIS, K. M.; MANGHAM, A. N.; HAMERS, R. J.; HEIDEMAN, W.; PETERSON, R. E.; PEDERSEN, J. A. Toxicity of Oxidatively Degraded Quantum Dots to Developing Zebrafish (*Danio rerio*). **Environ Sci Technol.**, v. 47, n. 16, p. 9132-9139, 2013.

WOLSKA, E.; KASZEWSKI, J.; KIEŁBIK, P.; GRZYB, J.; GODLEWSKI, M.M.; GODLEWSKI, M.. Rare earth activated ZnO nanoparticles as biomarkers. **Opt Mater**, v. 36, n. 10, p. 1655-1659, 2014.

WOOD, A.; GIERSIG, M.; HILGENDORFF, M.; VILAS-CAMPOS, A.; LIZ-MARZÁN, L. M.; MULVANEY, P.. Size Effects in ZnO: The Cluster to Quantum Dot Transition. **Aust J Chem**, v. 56, n. 10, p. 1051-1057, 2003.

WU, Y. L.; FU, S.; TOK, A. I.; ZENG, X. T.; LIM, C. S.; KWEK, L. C.; BOEY, F. C. A dual-colored bio-marker made of doped ZnO nanocrystals. **Nanotechnology**, v. 19, n. 34, p.1-9, 2008.

XIONG, H.-M. XU, Y.; REN, Q. G.; XIA, Y. Y. Stable Aqueous ZnO@Polymer Core–Shell Nanoparticles with Tunable Photoluminescence and Their Application in Cell Imaging. **J Am Chem Soc**, v. 130, n. 24, p. 7522-7523, 2008.

XIONG, H.-M. Photoluminescent ZnO nanoparticles modified by polymers. **J Mater Chem**, v. 20, n. 21, p. 4251-4262, 2010.

YAN, C.; TANG, F.; LI, L.; LI, H.; HUANG, X.; CHEN, D.; MENG, X.; REN, J. Synthesis of Aqueous CdTe/CdS/ZnS Core/shell/shell Quantum Dots by a Chemical Aerosol Flow Method. **Nanoscale Res Lett**, v. 5, n. 1, p. 189-194, 2009.

YANG, J.;YAO, M. H.; WEN, L.; SONG, J. T.; ZHANG, M. Z.; ZHAO, Y. D.; LIU, B. Multifunctional quantum dot-polypeptide hybrid nanogel for targeted imaging and drug delivery. **Nanoscale**, v. 6, n. 19, p. 11282-11292, 2014.

YANG, Y.;JIN, Y.; HE, H.; WANG, Q.; TU, Y.; LU, H.; YE, Z. Dopant-Induced Shape Evolution of Colloidal Nanocrystals: The Case of Zinc Oxide. **J Am Chem Soc**, v. 132, n. 38, p. 13381-13394, 2010.

YANG Y., LV, S-Y. YU, B., XU, S., SHEN, J., ZHAO, T., ZHANG, H. Hepatotoxicity assessment of Mn-doped ZnS quantum dots after repeated administration in mice. **Int J Nanomedicine**, v. 10, p. 5787-5796, 2015.

YHEE, J. Y.; LEE, S.; KIM, K. Advances in targeting strategies for nanoparticles in cancer imaging and therapy. **Nanoscale**, v. 6, n. 22, p. 13383-13390, 2014.

YIN, Q.;JIN, X.;YANG, G.;JIANG, C.;SONGA, Z.; SUN, G. Biocompatible folate-modified Gd<sup>3+</sup>/Yb<sup>3+</sup>-doped ZnO nanoparticles for dualmodal MRI/CT imaging. **RSC Adv**, v. 4, n. 96, p. 53561-53569, 2014.

YOUSEFI, R.; ZAK, A. K.; JAMALI-SHEINI, F. Growth, X-ray peak broadening studies, and optical properties of Mg-doped ZnO nanoparticles. **Mater Sci Semicond Process**, v. 16, n. 3, p. 771-777, 2013.

YU, M. K.; PARK, J.; JON, S. Targeting Strategies for Multifunctional Nanoparticles in Cancer Imaging and Therapy. **Theranostics**, v. 2, n. 1, p. 3-44, 2012.

LV, Y., XIAO, W. LI, W., XUE, J., DING, J. Controllable synthesis of ZnO nanoparticles with high intensity visible photoemission and investigation of its mechanism. **Nanotechnology**, v. 24, n. 17, p. 175702:1-10, 2013.

ZHANG, Z.H., WANG, X., XU, J.B., MULLER, S., RONNING, C. & LI, Q. Evidence of intrinsic ferromagnetism in individual dilute magnetic semiconductor nanostructures. **Nature Nanotech**. v.4, p. 523-527 , 2009.

ZHANG, H-J., XIONG, H-M., REN, Q-G., XIA, Y-Y., KONG, J-L. ZnO@silica core-shell nanoparticles with remarkable luminescence and stability in cell imaging. **J Mater Chem**, v. 22, p. 13159-13165, 2012.

ZHANG, Z-Y., XU, Y-D., MA, Y-Y., QIU, L-L., WANG, Y., KONG, J-L., XIONG, H-M. Biodegradable ZnO@polymer Core-Shell Nanocarriers: pH-Triggered Release of Doxorubicin In Vitro. **Angew Chem Int Ed Engl**, v. 52, p. 4127-4131, 2013.

## ***Chapter I - Bibliography***

---

ZHANG, Y.; HUANG, Y.; LI, S. Polymeric Micelles: Nanocarriers for Cancer-Targeted Drug Delivery. **AAPS PharmSciTech**, New York, v. 15, n. 4, p. 862-871, 2014.

ZHAO, L.-H.; ZHANG, R.; ZHANG, J.; SUN, S.-Q. Synthesis and characterization of biocompatible ZnO nanoparticles. **CrystEngComm**, v. 14, n. 3, p. 945-950, 2012.

ZHOU, R.; LI, M.; WANG, S.; WU, P.; WU, L.; HOU, X. Low-toxic Mn-doped ZnSe@ZnS quantum dots conjugated with nano-hydroxyapatite for cell imaging. **Nanoscale**, v. 6, n. 23, p. 14319-14325, 2014.

#### II.4. REFERENCES

BANCOS, S.; STEVENS, D. L.; TYNER, K. M. Effect of silica and gold nanoparticles on macrophage proliferation, activation markers, cytokine production, and phagocytosis in vitro. **Int J Nanomedicine**, v. 10, p. 183-206, 2015.

BRIOIS, V.; SERRINI, P.; CHIAVACCI, L.; PULCINELLI, S. H.; SANTILLI, C. V. EXAFS spectroscopy of nanocrystalline materials. In: NETWORK, T. R. (Ed.). **Recent Research and Development of Non-Crystalline Solids**. Kerala, India, v.1, 2001. p.21-35. ISBN 81-7895-028-6.

BRUS, L. E. A simple model for the ionization potential, electron affinity, and aqueous redox potentials of small semiconductor crystallites. **J Chem Phys**, v. 79, n. 11, p. 5566-5571, 1983.

CHEMIN, C.; PÉAN, J. M.; BOURGAUX, C.; PABST, G.; WÜTHRICH, P.; COUVREUR, P.; OLLIVON, M. Supramolecular organization of S12363-liposomes prepared with two different remote loading processes. **Biochim Biophys Acta**, v. 1788, n. 5, p. 926-935, 2009.

CHUKWUOCHA, E.; ONYEAJU, M.; HARRY, T. Theoretical Studies on the Effect of Confinement on Quantum Dots Using the Brus Equation. **World Journal of Condensed Matter Physics**, v. 2, n. 2, p. 96-100, 2012.

CRAIEVICH, A. F. **Handbook of Sol-Gel Science and Technology**; Norwell: Sakka, S., Almeida, R., Eds., 2005. vol.2, chapter II, p 161-189.

CROSBY, G. A.; DEMAS, J. N. Measurement of photoluminescence quantum yields. Review. **J Phys Chem**, v. 75, n. 8, p. 991-1024, 1971.

DONG, Y.-D.; BOYD, B. J. Applications of X-ray scattering in pharmaceutical science. **Int J Pharm**, v. 417, n. 1-2, p. 101-111, 2011.

GRUNWALDT, J.-D.; BAIKER, A. In situ spectroscopic investigation of heterogeneous catalysts and reaction media at high pressure. **Phys Chem Chem Phys**, v. 7, n. 20, p. 3526-3539, 2005.

INOBE, T.; TAKAHASHI, K.; MAKI, K.; ENOKI, S.; KAMAGATA, K.; KADOOKA, A.; ARAI, M.; KUWAJIMA, K. Asymmetry of the GroEL-GroES Complex under Physiological Conditions as Revealed by Small-Angle X-Ray Scattering. **Biophys J**, v. 94, n. 4, p. 1392-1402, 2008.

KOHLBRECHER, J.; BRESSLER, I. **SASfit**. Paul Scherrer Institut, Villigen, Switzerland. 0.94.1 2014.

LEPELTIER, E., BOURGAXU, C., COUVREUR P. Nanoprecipitation and the “Ouzo effect”: Application to drug delivery devices. **Adv Drug Deliv Rev**, v.71, p. 86-97, 2014.

MANAIA, E. B.;KAMINSKI, R. C.; DE OLIVEIRA, A. G.; CORRÊA, M. A.; CHIAVACCI, L. A. Multifunction hexagonal liquid-crystal containing modified surface TiO<sub>2</sub> nanoparticles and terpinen-4-ol for controlled release. **Int J Nanomedicine**, v. 10, p. 811-819, 2015.

MEULENKAMP, E. A. Synthesis and Growth of ZnO Nanoparticles. **J Phys Chem B**, v. 102, n. 29, p. 5566-5572, 1998.

MULET, X.; BOYD, B. J.; DRUMMOND, C. J. Advances in drug delivery and medical imaging using colloidal lyotropic liquid crystalline dispersions. **J Colloid Interface Sci**, v. 393, p. 1-20, 2013.

NASCIMENTO, T. L.; HILLAIREAU, H.; NOIRAY, M.; BOURGAUX, C.; ARPICCO, S.; PEHAU-ARNAUDET, G.; TAVERNA, M.; COSCO, D.; TSAPIS, N.; FATTAL, E. Supramolecular Organization and siRNA Binding of Hyaluronic Acid-Coated Lipoplexes for Targeted Delivery to the CD44 Receptor. **Langmuir**, v. 31, n. 41, p. 11186-11194, 2015.

NEDELIJKOVIC, J. M.; PATEL, R. C.;KAUFMAN, P.;JOYCE-PRUDEN, C.;O'LEARY, N. Synthesis and optical properties of quantum-sized metal sulfide particles in aqueous solution. **J Chem Educ**, v. 70, n. 4, p. 342, 1993.

PETOUKHOV, M. V.; SVERGUN, D. I. Applications of small-angle X-ray scattering to biomacromolecular solutions. **Int J Biochem Cell Biol**, v. 45, n. 2, p. 429-437, 2013.

SPANHEL, L.; ANDERSON, M. A. Semiconductor clusters in the sol-gel process: quantized aggregation, gelation, and crystal growth in concentrated zinc oxide colloids. **J Am Chem Soc**, v. 113, n. 8, p. 2826-2833, 1991.

SUN, L.-W.; SHI, H.-Q.; LI, W.-N.; XIAO, H.-M.; FU, S.-Y.; CAO, X.-Z.; LI, Z.-X.. Lanthanum-doped ZnO quantum dots with greatly enhanced fluorescent quantum yield. **J Mater Chem**, v. 22, n. 17, p. 8221-8227, 2012.

WEST, A. R. **Solid State Chemistry and Its Applications**. New York: John Wiley and Sons, 1992.

WILLIAMS, D. B., CARTER, C. B. **Transmission Electron Microscopy. A Textbook for Materials Science.** New York: Springer Science+Business Media, 2009. p. 49.

YANO, J.; YACHANDRA, V. K. X-ray absorption spectroscopy. **Photosynthesis Research**, v. 102, n. 2-3, p. 241-254, 2009.

### III.5. REFERENCES

BIAN, S.-W.; MUDUNKOTUWA, I. A.; RUPASINGHE, T.; GRASSIAN, V. H. Aggregation and Dissolution of 4 nm ZnO Nanoparticles in Aqueous Environments: Influence of pH, Ionic Strength, Size, and Adsorption of Humic Acid. **Langmuir**, v. 27, n. 10, p. 6059-6068, 2011.

BRIOIS, V. GIORGETTI, C.H.; BAUDELET, F.; BLANCHANDIN, S.; TOKUMOTO, M. S.; PULCINELLI, S. H.; SANTILLI, C. V. Dynamical Study of ZnO Nanocrystal and Zn-HDS Layered Basic Zinc Acetate Formation from Sol-Gel Route. **J Phys Chem C Nanomater Interfaces**, v. 111, n. 8, p. 3253-3258, 2007.

BRUS, L. E. A simple model for the ionization potential, electron affinity, and aqueous redox potentials of small semiconductor crystallites. **J Chem Phys**, v. 79, n. 11, p. 5566-5571, 1983.

CAETANO, B. L. SANTILLI, C. V.; MENEAU, F.; BRIOIS, V.; PULCINELLI, S. H. In Situ and Simultaneous UV-vis/SAXS and UV-vis/XAFS Time-Resolved Monitoring of ZnO Quantum Dots Formation and Growth. **J Phys Chem C Nanomater Interfaces**, v. 115, n. 11, p. 4404-4412, 2011.

CASSETTE, E.; PONS, T.; BOUET, C.; HELLE, M.; BEZDETNYA, L.; MARCHAL, F.; DUBERTRET, B. Synthesis and Characterization of Near-Infrared Cu-In-Se/ZnS Core/Shell Quantum Dots for In vivo Imaging. **Chem Mater**, v. 22, n. 22, p. 6117-6124, 2010.

CHEN, O.; ZHAO, J.; CHAUHAN, V. P.; CUI, J.; WONG, C.; HARRIS, D. K.; WEI, H.; HAN, H. S.; FUKUMURA, D.; JAIN, R. K.; BAWENDI, M. G. Compact high-quality CdSe-CdS core-shell nanocrystals with narrow emission linewidths and suppressed blinking. **Nat Mater**, v. 12, n. 5, p. 445-451, 2013.

CURCIO, A. L.; BERNARDI, M. I. B.; MESQUITA, A. Local structure and photoluminescence properties of nanostructured Zn<sub>1-x</sub>Mn<sub>x</sub>S material. **Phys Status Solidi Rapid Res Lett.**, v. 12, n. 12, p. 1367-1371, 2015.

DABBOUSI, B. O.; RODRIGUEZ-VIEJO, J.; MIKULEC, F. V.; HEINE, J. R.; MATTOUSSI, H.; OBER, R.; JENSEN, K. F.; BAWENDI, M. G. (CdSe)<sub>2</sub>ZnS Core-Shell Quantum Dots: Synthesis and Characterization of a Size Series of Highly Luminescent Nanocrystallites. **J Phys Chem B**, v. 101, n. 46, p. 9463-9475, 1997.

DAVID, C. A.; GALCERAN, J.; REY-CASTRO, C.; PUY, J.; COMPANYS, E.; SALVADOR, J.; MONNÉ, J.; WALLACE, R.; VAKOUROV, A. Dissolution Kinetics and Solubility of ZnO Nanoparticles Followed by AGNES. **J Phys Chem C Nanomater Interfaces**, v. 116, n. 21, p. 11758-11767, 2012.

GENG, J.; LIU, B.; XU, L.; HU, F. N.; ZHU, J. J. Facile Route to Zn-Based II–VI Semiconductor Spheres, Hollow Spheres, and Core/Shell Nanocrystals and Their Optical Properties. **Langmuir**, v. 23, n. 20, p. 10286-10293, 2007.

GHOSH CHAUDHURI, R.; PARIA, S. Core/Shell Nanoparticles: Classes, Properties, Synthesis Mechanisms, Characterization, and Applications. **Chem Rev**, v. 112, n. 4, p. 2373-2433, 2011.

GUINIER, A.; FOURNET, G. **Small Angle Scattering of X-rays**. New-York: Wiley, 1955.

ISNAENI; KIM, K. H.; NGUYEN, D. L.; LIM, H.; NGA, P. T.; CHO, Y.-H. Shell layer dependence of photoblinking in CdSe/ZnSe/ZnS quantum dots. **Appl Phys Lett**, v. 98, n. 1, p. 012109-3, 2011.

JIA, Z.; MISRA, R. D. K. Tunable ZnO quantum dots for bioimaging: synthesis and photoluminescence. **Mater Technol**, v. 28, n. 4, p. 221-227, 2013.

LIM, J. H.; KANG, C. K.; KIM, K. K.; PARK, I. K.; HWANG, D. K.; PARK, S. J. UV Electroluminescence Emission from ZnO Light-Emitting Diodes Grown by High-Temperature Radiofrequency Sputtering. **Adv Mater**, v. 18, n. 20, p. 2720-2724, 2006.

LIU, K.; SAKURAI, M.; AONO, M. ZnO-Based Ultraviolet Photodetectors. **Sensors (Basel, Switzerland)**, v. 10, n. 9, p. 8604-8634, 2010.

LIU, L.; CHEN, Y.; GUO, T.; ZHU, Y.; SU, Y.; JIA, C.; WEI, M.; CHENG, Y. Chemical Conversion Synthesis of ZnS Shell on ZnO Nanowire Arrays: Morphology Evolution and Its Effect on Dye-Sensitized Solar Cell. **ACS Appl Mater Interfaces**, v. 4, n. 1, p. 17-23, 2011.

LUO, J.; ZHAO, S.; WU, P.; ZHANG, K.; PENG, C.; ZHENG, S. Synthesis and characterization of new Cd-doped ZnO/ZnS core-shell quantum dots with tunable and highly visible photoluminescence. **J Mater Chem C**, v. 3, n. 14, p. 3391-3398, 2015.

MATSUYAMA, K.; IHSAN, N.; IRIE, K.; MISHIMA, K.; OKUYAMA, T.; MUTO, H. Bioimaging application of highly luminescent silica-coated ZnO-nanoparticle quantum dots with biotin. **J Colloid Interface Sci**, v. 399, p. 19-25, 2013.

MEHTA, S. K.; KUMAR, S.; CHAUDHARY, S.; BHASIN, K. K.; GRADZIELSKI, M. Evolution of ZnS Nanoparticles via Facile CTAB Aqueous Micellar Solution Route: A Study on Controlling Parameters. **Nanoscale Res Lett**, v. 4, n. 1, p. 17-28, 2008.



MEULENKAMP, E. A. Size Dependence of the Dissolution of ZnO Nanoparticles. **J Phys Chem B**, v. 102, n. 40, p. 7764-7769, 1998.

MOUSSODIA, R.-O, BALAN, L., MERLIN, C., MUSTIN, C., SCHNEIDER, R. Biocompatible and stable ZnO quantum dots generated by functionalization with siloxane-core PAMAM dendrons. **J Mater Chem**, v. 20, p. 1147-1155, 2010.

NAM, W.; LIM, Y. S.; SEO, W.-S.; CHO, H. K.; LEE, J. Y. Control of the shell structure of ZnO–ZnS core-shell structure. **J Nanopart Res**, v. 13, n. 11, p. 5825-5831, 2011.

PANDA, S. K.; DEV, A.; CHAUDHURI, S. Fabrication and luminescent properties of c-axis oriented ZnO-ZnS core-shell and ZnS nanorod arrays by sulfidation of aligned ZnO nanorod arrays. **J Phys Chem C Nanomater Interfaces**, v. 111, n. 13, p. 5039-5043, 2007.

REISS, P.; PROTÈRE, M.; LI, L. Core/Shell Semiconductor Nanocrystals. **Small**, v. 5, n. 2, p. 154-168, 2009.

SADOLLAHKHANI, A.; KAZEMINEZHAD, I.; LU, J.; NUR, O.; HULTMAN, L.; WILLANDER, M. Synthesis, structural characterization and photocatalytic application of ZnO@ZnS core-shell nanoparticles. **RSC Adv**, v. 4, n. 70, p. 36940-36950, 2014.

SHARMA, M.; KUMAR, S.; PANDEY, O. P. Study of energy transfer from capping agents to intrinsic vacancies/defects in passivated ZnS nanoparticles. **J Nanopart Res**, v. 12, n. 7, p. 2655-2666, 2010.

SHARMA, S.; CHAWLA, S. Enhanced UV emission in ZnO/ZnS core shell nanoparticles prepared by epitaxial growth in solution. **Electronic Materials Letters**, v. 9, n. 3, p. 267-271, 2013.

SHUAI, X. M.; SHEN, W. Z. A Facile Chemical Conversion Synthesis of ZnO/ZnS Core/Shell Nanorods and Diverse Metal Sulfide Nanotubes. **J Phys Chem C Nanomater Interfaces**, v. 115, n. 14, p. 6415-6422, 2011.

SOOKHAKIAN, M.; AMIN, Y. M.; BASIRUN, W. J.; TAJABADI, M. T.; KAMARULZAMAN, N. Synthesis, structural, and optical properties of type-II ZnO–ZnS core–shell nanostructure. **J Lumin**, v. 145, n. 0, p. 244-252, 2014.

THUY, U. T. D., LIEM, N. Q. Transition from type-I to type-II CdTe/CdS core/shell quantum dots synthesized in water at low temperature. **J Nanosci Nanotechnol**, v. 4, n. 4, p. 045010, 2013.

TOKUMOTO, M. S., BRIOS, V.; SANTILLI, C. V.; PULCINELLI, S. H. Preparation of ZnO Nanoparticles: Structural Study of the Molecular Precursor. **J Solgel Sci Technol**, v. 26, n. 1-3, p. 547-551, 2003.

VERMA, P.; PANDEY, A. C.; BHARGAVA, R. N. Synthesis and characterisation: Zinc oxide-sulfide nanocomposites. **Physica B Condens Matter**, v. 404, n. 21, p. 3894-3897, 2009.

WANG, X.; REN, X.; KAHEN, K.; HAHN, M. A.; RAJESWARAN, M.; MACCAGNANO-ZACHER, S.; SILCOX, J.; CRAGG, G. E.; EFROS, A. L.; KRAUSS, T. D. Non-blinking semiconductor nanocrystals. **Nature**, v. 459, n. 7247, p. 686-689, 2009a.

WANG, Y., GUO, Q., LIN, S., CHEN, B., ZHENG, D. Growth and properties of ZnO/ZnS core/shell nanostructures. **Journal of Physics: Conference Series**, v. 152, n. 1, p. 012018, 2009b.

WANG, L.;KANG, Y.;LIU, X.;ZHANG, S.;HUANG, W.;WANG, S.ZnO nanorod gas sensor for ethanol detection. **Sens Actuators B Chem**, v. 162, n. 1, p. 237-243, 2012.

WEST, A. R. **Solid State Chemistry and Its Applications**. New York: John Wiley and Sons 1992.

WU, D.; JIANG, Y.;YUAN, Y.;WU, J.;JIANG, K. ZnO-ZnS heterostructures with enhanced optical and photocatalytic properties. **J Nanopart Res**, v. 13, n. 7, p. 2875-2886, 2011.

XIONG, H.-M. Photoluminescent ZnO nanoparticles modified by polymers. **J Mater Chem**, v. 20, n. 21, p. 4251-4262, 2010.

XIONG, H.-X. ZnO Nanoparticles Applied to Bioimaging and Drug Delivery. **Adv Mater**, v. 25, n. 37, p. 5329-5335, 2013.

#### IV.5. REFERENCES

BAGALKOT, V.;ZHANG, L.; LEVY-NISSENBAUM, E.; JON, S.; KANTOFF, P. W.; LANGER, R.; FAROKHZAD, O. C. Quantum Dot–Aptamer Conjugates for Synchronous Cancer Imaging, Therapy, and Sensing of Drug Delivery Based on Bi-Fluorescence Resonance Energy Transfer. **Nano Lett**, v. 7, n. 10, p. 3065-3070, 2007.

BRINKER, C. J.; SCHERER, G. W. **Sol-Gel Sciences. The Physics and Chemistry of Sol-Gel Processing**. San Diego: Academic Press, Inc, p. 908, 1990.

BRUS, L. Electronic wave functions in semiconductor clusters: experiment and theory. **J Phys Chem**, v. 90, n. 12, p. 2555-2560, 1986.

BUONSANTI, R.; MILLIRON, D. J. Chemistry of Doped Colloidal Nanocrystals. **Chem Mater**, v. 25, n. 8, p. 1305-1317, 2013.

CAETANO, B. L. SANTILLI, C. V.; MENEAU, F.; BRIOIS, V.; PULCINELLI, S. H. In Situ and Simultaneous UV–vis/SAXS and UV–vis/XAFS Time-Resolved Monitoring of ZnO Quantum Dots Formation and Growth. **J Phys Chem CNanomater Interfaces**, v. 115, n. 11, p. 4404-4412, 2011.

CHANG, E.;THEKKEK, N.; YU, W. W.; COLVIN, V. L.; DREZEK, R.. Evaluation of Quantum Dot Cytotoxicity Based on Intracellular Uptake. **Small**, v. 2, n. 12, p. 1412-1417, 2006.

COHN, A. W.; KITTILSTVED, K. R.; GAMELIN, D. R. Tuning the Potentials of “Extra” Electrons in Colloidal n-Type ZnO Nanocrystals via Mg<sup>2+</sup> Substitution. **J Am Chem Soc**, v. 134, n. 18, p. 7937-7943, 2012.

CRAIEVICH, A. F. **Handbook of Sol-Gel Science and Technology**. Norwell, MA: Kluwer Publishers, p.161-189, 2005.

DING, R.;XU, C.;GU, B.;SHI, Z.; WANG, H.;BA, L.;XIAO, Z. Effects of Mg Incorporation on Microstructure and Optical Properties of ZnO Thin Films Prepared by Sol-gel Method. **J Mater Sci Technol**, v. 26, n. 7, p. 601-604, 2010.

FELBIER, P.;YANG, J.;THEIS, J.;LIPTAK, R. W.;WAGNER, A.;LORKE, A.;BACHER, G.;KORTSHAGEN, U.Highly Luminescent ZnO Quantum Dots Made in a Nonthermal Plasma. **Adv Funct Mater**, v. 24, n. 14, p. 1988-1993, 2014.

#### **Chapter IV – Surface modified Mg-doped ZnO QDs for biological imaging**

---

GHOSH, M.; RAYCHAUDHURI, A. K. Optical Properties of Mg-Substituted ZnO Nanoparticles Obtained by Solution Growth. **IEEE Trans Nanotechnol**, v. 10, n. 3, p. 555-559, 2011.

GUINIER, A.; FOURNET, G. **Small Angle Scattering of X-rays**. New-York: Wiley, 1955.

JIA, Z.; MISRA, R. D. K. Tunable ZnO quantum dots for bioimaging: synthesis and photoluminescence. **Mater Technol**, v. 28, n. 4, p. 221-227, 2013.

KLAINÉ, S. J.; ALVAREZ, P. J.; BATLEY, G. E.; FERNANDES, T. F.; HANDY, R. D.; LYON, D. Y.; MAHENDRA, S.; MCLAUGHLIN, M. J.; LEAD, J. R. Nanomaterials in the environment: Behavior, fate, bioavailability, and effects. **Environ Toxicol Chem**, v. 27, n. 9, p. 1825-1851, 2008.

KOLEVA, V.; STOILOVA, D. Infrared and Raman studies of the solids in the  $\text{Mg}(\text{CH}_3\text{COO})_2\text{-Zn}(\text{CH}_3\text{COO})_2\text{-H}_2\text{O}$  system. **J Mol Struct**, v. 611, n. 1-3, p. 1-8, 2002.

LAYEK, A.; DE, S.; THORAT, R.; CHOWDHURY, A. Spectrally Resolved Photoluminescence Imaging of ZnO Nanocrystals at Single-Particle Levels. **J Phys Chem Lett**, v. 2, n. 11, p. 1241-1247, 2011.

LEWINSKI, N.; COLVIN, V.; DREZEK, R. Cytotoxicity of Nanoparticles. **Small**, v. 4, n. 1, p. 26-49, 2008.

LIN, Y.-J.; WU, P.-H.; TSAI, C.-L.; LIU, C.-J.; LIN, Z.-R.; CHANG, H.-C.; LEE, C.-T. Effects of Mg incorporation on the optical properties of ZnO prepared by the sol-gel method. **J Appl Phys**, v. 103, p. 113709, 2008.

LIU, D.-P.; LI, G. D.; SU, Y.; CHEN, J. S. Highly Luminescent ZnO Nanocrystals Stabilized by Ionic-Liquid Components. **Angew Chem Int Ed Engl**, v. 45, n. 44, p. 7370-7373, 2006.

MICHALET, X.; PINAUD, F. F.; BENTOLILA, L. A.; TSAY, J. M.; DOOSE, S.; LI, J. J.; SUNDARESAN, G.; WU, A. M.; GAMBHIR, S. S.; WEISS, S. Quantum Dots for Live Cells, in Vivo Imaging, and Diagnostics. **Science**, v. 307, n. 5709, p. 538-544, 2005.

MOUSSODIA, R.-O, BALAN, L., MERLIN, C., MUSTIN, C., SCHNEIDER, R. Biocompatible and stable ZnO quantum dots generated by functionalization with siloxane-core PAMAM dendrons. **J Mater Chem**, v. 20, p. 1147-1155, 2010.

#### ***Chapter IV – Surface modified Mg-doped ZnO QDs for biological imaging***

---

NORBERG, N. S.; KITTILSTVED, K. R.; AMONETTE, J. E.; KUKKADAPU, R. K.; SCHWARTZ, D. A.; GAMELIN, D. R. Synthesis of Colloidal Mn<sup>2+</sup>:ZnO Quantum Dots and High-TC Ferromagnetic Nanocrystalline Thin Films. **J Am Chem Soc**, v. 126, n. 30, p. 9387-9398, 2004.

PARK, J.-H.; VON MALTZAHN, G.; RUOSLAHTI, E.; BHATIA, S. N.; SAILOR, M. J. Micellar Hybrid Nanoparticles for Simultaneous Magnetofluorescent Imaging and Drug Delivery. **Angew Chem Int Ed Engl**, v. 47, n. 38, p. 7284-7288, 2008.

SCHWARTZ, D. A.; NORBERG, N. S.; NGUYEN, Q. P.; PARKER, J. M.; GAMELIN, D. R. Magnetic Quantum Dots: Synthesis, Spectroscopy, and Magnetism of Co<sup>2+</sup>- and Ni<sup>2+</sup>-Doped ZnO Nanocrystals. **J Am Chem Soc**, v. 125, n. 43, p. 13205-13218, 2003.

SU, Y.; HE, Y.; LU, H.; SAI, L.; LI, Q.; LI, W.; WANG, L.; SHEN, P.; HUANG, Q.; FAN, C. The cytotoxicity of cadmium based, aqueous phase – Synthesized, quantum dots and its modulation by surface coating. **Biomaterials**, v. 30, n. 1, p. 19-25, 2009.

TIAN, B.; AL-JAMAL, W. T.; AL-JAMAL, K. T.; KOSTARELOS, K. Doxorubicin-loaded lipid-quantum dot hybrids: Surface topography and release properties. **Int J Pharm**, v. 416, n. 2, p. 443-447, 2011.

VAN DIJKEN, A.; MEULENKAMP, E. A.; VANMAEKELBERGH, D.; MEIJERINK, A. The Kinetics of the Radiative and Nonradiative Processes in Nanocrystalline ZnO Particles upon Photoexcitation. **J Phys Chem B**, v. 104, n. 8, p. 1715-1723, 2000.

VIJAYALAKSHMI, K.; KARTHICK, K. Influence of Mg doping on the microstructure and PL emission of wurtzite ZnO synthesized by microwave processing. **J Mater Sci Mater Electron**, v. 24, n. 6, p. 2067-2071, 2013.

WANG, C.; GAO, X.; SU, X. In vitro and in vivo imaging with quantum dots. **Anal Bioanal Chem**, v. 397, n. 4, p. 1397-1415, 2010.

WEST, A. R. **Solid State Chemistry and Its Applications**. New York: John Wiley and Sons 1992.

XIE, J.; LEE, S.; CHEN, X. Nanoparticle-based theranostic agents. **Adv Drug Deliv Rev**, v. 62, n. 11, p. 1064-1079, 2010.

XIONG, H.-M.; SHCHUKIN, D. G.; MÖHWALD, H.; XU, Y.; XIA, Y. Y. Sonochemical Synthesis of Highly Luminescent Zinc Oxide Nanoparticles Doped with Magnesium(II). **Angewandte Chemie**, v. 121, n. 15, p. 2765-2769, 2009.

**Chapter IV – Surface modified Mg-doped ZnO QDs for biological imaging**

---

XIONG, H.-M. Photoluminescent ZnO nanoparticles modified by polymers. **J Mater Chem**, v. 20, n. 21, p. 4251-4262, 2010.

XIONG, H.-M. ZnO Nanoparticles Applied to Bioimaging and Drug Delivery. **Adv Mater**, v. 25, p. 5329–5335, 2013.

XU, X.;XU, C.;WANG, X.;LIN, Y.;DAI, J.;HU, J. Control mechanism behind broad fluorescence from violet to orange in ZnO quantum dots. **CrystEngComm**, v. 15, n. 5, p. 977-981, 2013.

YANG, Y.;JIN, Y.; HE, H.; WANG, Q.; TU, Y.; LU, H.; YE, Z. Dopant-Induced Shape Evolution of Colloidal Nanocrystals: The Case of Zinc Oxide. **J Am Chem Soc**, v. 132, n. 38, p. 13381-13394, 2010.

YOUSEFI, R.;SHEINI, F. J.; MUHAMAD,M. R.;MORED, M. A. Characterization and field emission properties of ZnMgO nanowires fabricated by thermal evaporation process. **Solid State Sciences**, v. 12, n. 7, p. 1088-1093, 2010.

YOUSEFI, R.; KAMALUDDIN, B. Fabrication and characterization of ZnO and ZnMgO nanostructures grown using a ZnO/ZnMgO compound as the source material. **Appl Surf Sci**, v. 256, n. 1, p. 329-334, 2009.

YOUSEFI, R.; ZAK, A. K.; JAMALI-SHEINI, F. Growth, X-ray peak broadening studies, and optical properties of Mg-doped ZnO nanoparticles. **Mater Sci Semicond Process**, v. 16, n. 3, p. 771-777, 2013.

ZHANG, L.;YIN, L.;WANG, C.;LUN, N.;QI, Y.;XIANG, D. Origin of Visible Photoluminescence of ZnO Quantum Dots: Defect-Dependent and Size-Dependent. **J Phys Chem CNanomater Interfaces**, v. 114, n. 21, p. 9651-9658, 2010.

#### V.4. REFERENCES

ABED, N.; COUVREUR, P. Nanocarriers for antibiotics: A promising solution to treat intracellular bacterial infections. **Int J Antimicrob Agents**, v. 43, p. 485-496.

ADEREM, A.; UNDERHILL, D. M. MECHANISMS OF PHAGOCYTOSIS IN MACROPHAGES. **Annu Rev Immunol**, v. 17, n. 1, p. 593-623, 1999.

AL-JAMAL, W. T.; AL-JAMAL, K. T.; TIAN, B.; LACERDA, L.; BOMANS, P. H.; FREDERIK, P. M.; KOSTARELOS, K. Lipid–Quantum Dot Bilayer Vesicles Enhance Tumor Cell Uptake and Retention in Vitro and in Vivo. **ACS Nano**, v. 2, n. 3, p. 408-418, 2008.

DUBERTRET, B.; SKOURIDES, P.; NORRIS, D. J.; NOIREAUX, V.; BRIVANLOU, A. H.; LIBCHABER, A. In Vivo Imaging of Quantum Dots Encapsulated in Phospholipid Micelles. **Science**, v. 298, n. 5599, p. 1759-1762, 2002.

GARCÍA, I.; SÁNCHEZ-IGLESIAS, A.; HENRIKSEN-LACEY, M.; GRZELCZAK, M.; PENADÉS, S.; LIZ-MARZÁN, L. M. Glycans as Biofunctional Ligands for Gold Nanorods: Stability and Targeting in Protein-Rich Media. **J Am Chem Soc**, v. 137, n. 10, p. 3686-3692, 2015.

GOPALAKRISHNAN, G.; DANELON, C.; IZEWSKA, P.; PRUMMER, M.; BOLINGER, P. Y.; GEISSBÜHLER, I.; DEMURTAS, D.; DUBOCHET, J.; VOGEL, H. Multifunctional Lipid/Quantum Dot Hybrid Nanocontainers for Controlled Targeting of Live Cells. **Angew Chem Int Ed Engl**, v. 45, n. 33, p. 5478-5483, 2006.

HILLAIREAU, H.; COUVREUR, P. Nanocarriers' entry into the cell: relevance to drug delivery. **Cell Mol Life Sci**, v. 66, n. 17, p. 2873-2896, 2009.

JAULIN, N.; APPEL, M.; PASSIRANI, C.; BARRATT, G.; LABARRE, D. Reduction of the Uptake by a Macrophagic Cell Line of Nanoparticles Bearing Heparin or Dextran Covalently Bound to Poly(methyl methacrylate). **J Drug Target**, v. 8, n. 3, p. 165-172, 2000.

JOHANSSON, M.; HANSSON, P.; EDWARDS, K. Spherical Micelles and Other Self-Assembled Structures in Dilute Aqueous Mixtures of Poly(Ethylene Glycol) Lipids. **J Phys Chem B**, v. 105, n. 35, p. 8420-8430, 2001.

LEPELTIER, E.; BOURGAUX, C.; COUVREUR, P. Nanoprecipitation and the “Ouzo

*Chapter V – Incorporation of QDs in lipid-based nanocarriers: Preliminary results*

---

effect”: Application to drug delivery devices. **Adv Drug Deliv Rev**, v. 71, p. 86-97, 2014.

SALEM, I. I.; FLASHER, D. L.; DÜZGÜNEŞ, N. Liposome-Encapsulated Antibiotics1. In: (Ed.). **Methods Enzymol**, 2005. v. 391, p.261-291.

SCHROEDER, J. E.; SHWEKY, I.; SHMEEDA, H.; BANIN, U.; GABIZON, A. Folate-mediated tumor cell uptake of quantum dots entrapped in lipid nanoparticles. **J Control Release**, v. 124, n. 1–2, p. 28-34, 2007.

WI, H. S.; KIM, S. J.; LEE, K.; KIM, S. M.; YANG, H. S.; PAK, H. K. Incorporation of quantum dots into the lipid bilayer of giant unilamellar vesicles and its stability. **Colloids Surf B Biointerfaces**, v. 97, n. 0, p. 37-42, 2012.



# CHAPTER VI

## Final conclusions and perspectives

## **Chapter VI – Final conclusions and perspectives**

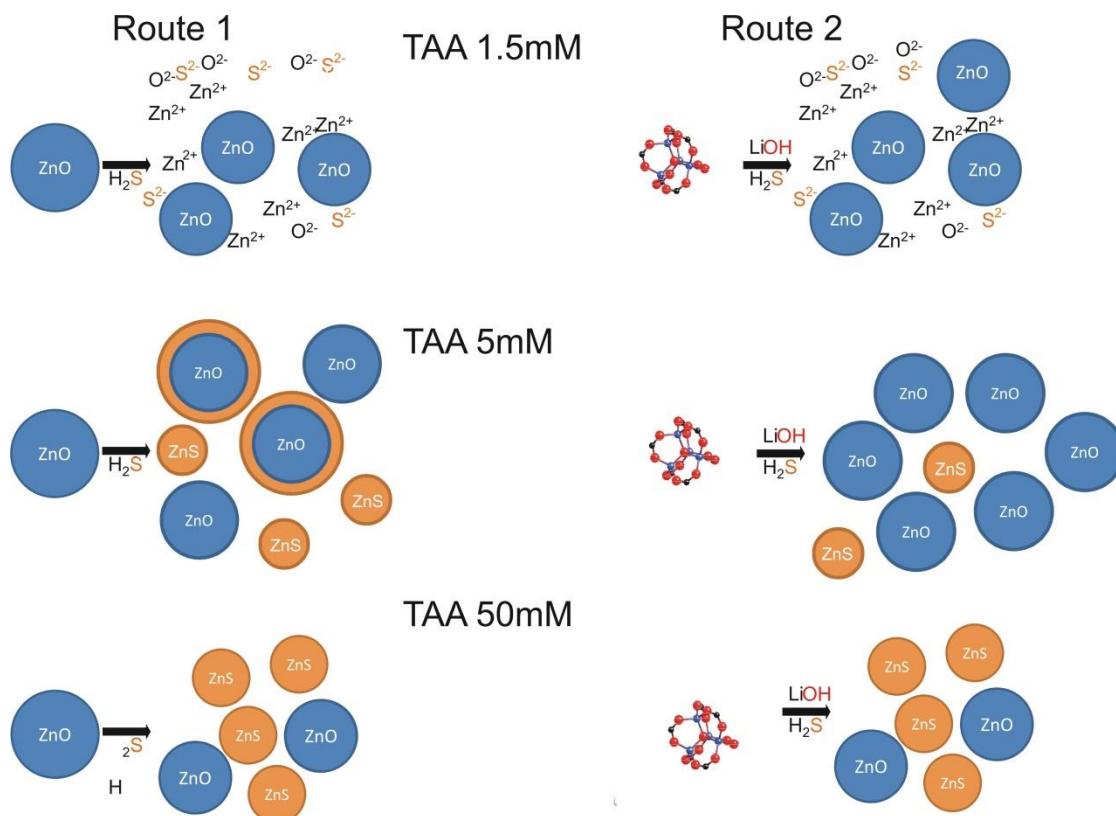
### **VI.1. Final conclusions**

The aim of this thesis was to explore ZnO based QDs as bioimaging agents due to their promising photoluminescent properties, when synthesized via sol-gel route, and low toxicity compared to the usual QDs, which contain heavy metals such as Cd, Pb, etc.

In a first step, attempts were made to improve the photoluminescence properties of ZnO QDs by synthesizing ZnO/ZnS core-shell QDs and doping ZnO QDs with Mg<sup>2+</sup> ions. Hereafter, QD surface modification was achieved for later incorporation in lipid based nanocarriers. Finally, the study of the structure, stability, photoluminescence properties and cell internalization of lipid nanocarriers loaded with QDs was carried out.

We could monitor the reactions tentatively used for obtaining ZnO/ZnS core-shell QDs and characterize the final products. We could observe that a small amount of TAA in the reaction medium was not sufficient to produce ZnS; an intermediate amount of TAA led to the formation of both species (ZnO and ZnS); and higher quantities of TAA gave mainly rise to ZnS nanoparticles. Figure VI.1 shows schematically the final products starting from either ZnAc precursor or ZnO colloidal suspensions mixed with three different TAA concentrations. The samples obtained in each reaction could be characterized by UV-vis, XRD and XAS techniques; however, it is noteworthy that only XAS allowed identifying core-shell structure when the reaction proceeded in ZnO colloidal suspension mixed with TAA 5 mM (Route1).

**Figure VI.1.** Schematical final products obtained in the reactions starting from ZnO colloidal suspensions (Route 1) and ZnAc precursor (Route 2) using three TAA concentrations (1.5, 5 and 50mM).

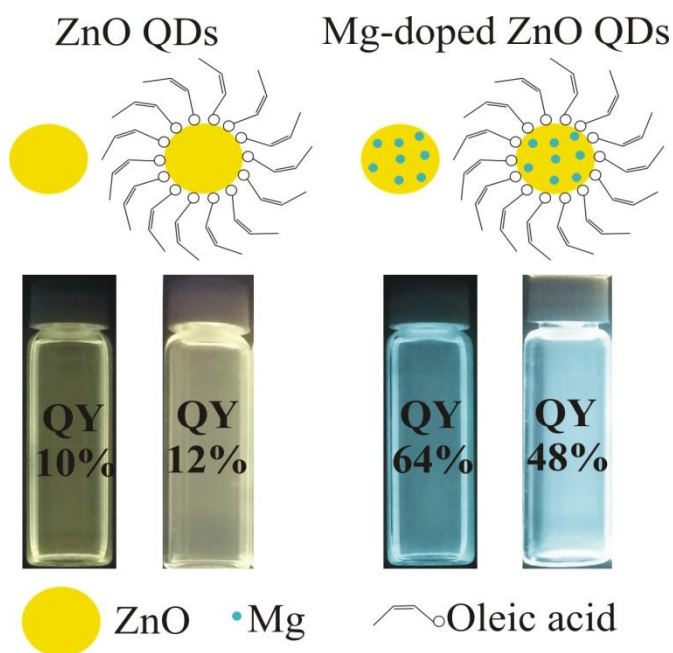


ZnO/ZnS QDs showed a rather weak photoluminescence in the visible range, compared to ZnO QDs, without displaying a significantly increased emission in the UV range. Therefore, doping of ZnO QDs with Mg ions was performed in an attempt to optimize their luminescence.

Mg-doped ZnO QDs were synthesized, preserving the wurtzite lattice of ZnO. The higher was the amount of dopant incorporated into ZnO structure, smaller was the size of nanoparticles. Mg ions incorporated into ZnO QDs strongly changed their growth, preventing the formation of fractal aggregates. We could increase the QY of ZnO QDs six times by using 20 mol% (nominal concentration) of  $\text{Mg}^{2+}$  ions in the reaction medium. The modification of their surface was also required to incorporate them into lipid-based nanocarriers. The ZnO and  $\text{Zn}_{0.8}\text{Mg}_{0.2}\text{O}$  QDs could be successfully capped by oleic acid (OA), forming stable colloidal dispersions in chloroform and toluene and keeping strong visible luminescence. Figure VI.2 presents schematically the structures of ZnO and  $\text{Zn}_{0.8}\text{Mg}_{0.2}\text{O}$  QDs with and without OA

coating, their photographs and respective QY. This part of the work has already been published in the European Journal of Nanomedicine, 7(2): 109–120, 2015 (Annexe).

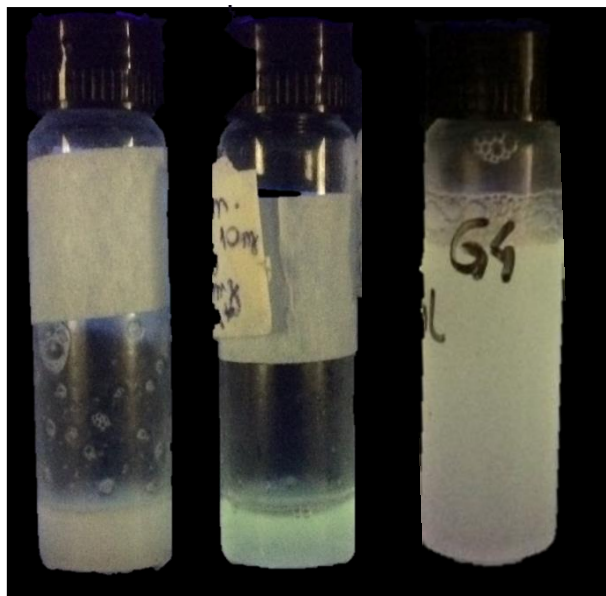
**Figure VI.2.** Schematical structures of ZnO and Zn<sub>0.8</sub>Mg<sub>0.2</sub>O QDs with and without OA capping, their photographs and respective QY.



Finally, we have tried to incorporate highly luminescent Zn<sub>0.8</sub>Mg<sub>0.2</sub>O and OA-Zn<sub>0.8</sub>Mg<sub>0.2</sub>O QDs into lipid-based nanocarriers.

Figure VI.3 shows examples of photographs of liposomes, DSPE-Peg based formulations and SLNs, loaded with QDs. As observed in this figure, liposomes presented lower luminescence compared to the DSPE-Peg formulation and SLN. SLNs were fairly stable in biological media, as shown by the absence of large aggregates. However, further investigations are needed to optimize the preparation and photoluminescence properties of the different nanocarriers for bioimaging applications.

**Figure VI.3.** Photographs of QDs loaded liposomes, a DSPE-Peg based formulation and an example of SLN (from left to right, respectively) under UV lamp.



## **VI.2. Perspectives**

ZnO/ZnS nanoparticles surface could be characterized by XPS, Zeta potential and isoelectric potential to confirm the modification of their surface by the ZnS shell deposition around the ZnO core.

Doping with  $Mg^{2+}$  ions widened the band gap of ZnO QDs and enhanced their visible luminescence. While studying Mg-doped ZnO QDs we could observe that  $Mg^{2+}$  ions interfere directly with the growth of the nanoparticles, inducing disorder in the ZnO lattice, decreasing the final size of the QDs and hindering their aggregation. However, we could not determine their location into ZnO QDs (in the core and/or at the surface). EXAFS and XANES spectra could be recorded at the Mg edge to identify the environment of Mg ions (nature and number of neighbors, distance between them). Indeed, no significant differences could be evidenced at the Zn edge between ZnO QDs and Mg-doped ZnO QDs. First experiments have been performed at LUCIA beamline at SOLEIL Synchrotron source. Work is in progress.

Regarding DPPC-based formulations which preserve the DPPC bilayer structure, atomic force microscopy (AFM) could be used to investigate the homogeneity of the repartition of QDs in the bilayers and the potential presence of QD aggregates. Further investigations are needed to better control the size and size distribution of the different nanocarriers, improve their luminescence and characterize their structure.

## *Chapter VI – Final Conclusions and perspectives*

---

For cell internalization studies, the limitations due to the cell auto-fluorescence phenomena might be overcome if ZnO QDs were excited at the optimal excitation wavelength with high intensity beam and short exposure time. Appropriate setups are available at the DISCO beamline at SOLEIL. Besides, the luminescent nanoparticle formulation, concentration and time of incubation with cells should be optimized.